Harou A.K Shahad is a Professor of Mechanical Engineering at Babylon University; IRAQ. His research interests are: combustion, renewable energies, pollution, hydrogen energy, thermodynamics, energy conversion and management, absorption cooling systems, internal combustion engines. Sabah Auda Abdul Ameer study in Mechanical Engineering at Babylon University; IRAQ. His research interests are: renewable energies, thermodynamics, energy conversion and management, absorption cooling systems.

Sabah Auda Abdul Ameer, Babylon University, College of Engineering; Dr. Haroun A.K Shahad, Babylon University, College of Engineering, Renewable Energy

978-613-9-86986-2

Master Thesis

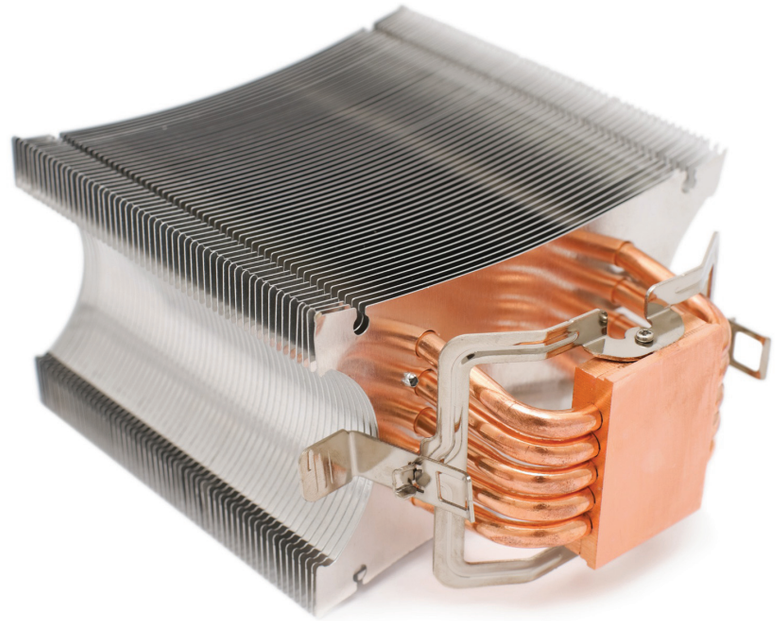

Sabah Auda
Haroun Abdul-kadhim Shahad

A Thermodynamic Study of Thermosiphon Loop Heat Pipe

Loop Heat Pipe

LAP LAMBERT Academic Publishing

Auda, Shahad

Sabah Auda
Haroun Abdul-kadhim Shahad

A Thermodynamic Study of Thermosiphon Loop Heat Pipe

Sabah Auda
Haroun Abdul-kadhim Shahad

A Thermodynamic Study of Thermosiphon Loop Heat Pipe

Loop Heat Pipe

LAP LAMBERT Academic Publishing

Imprint

Cover image: www.ingimage.com

Publisher:
LAP LAMBERT Academic Publishing
is a trademark of
International Book Market Service Ltd., member of OmniScriptum Publishing Group
17 Meldrum Street, Beau Bassin 71504, Mauritius

Printed at: see last page
ISBN: 978-613-9-86986-2

Zugl. / Approved by: Babylon,University of Babylon,Diss.,2007

Acknowledgements

Praise be to ***ALLAH***, Most Gracious, Most Merciful, who gave me the ability and desire to complete this research work.

I wish to express my cordial thanks and deepest gratitude to my supervisors ***Ass. Prof. Dr. Haroun A. K. Shahad*** and ***Ass. Prof. Dr. Tahseen A. Al-Hattab*** for their generous guidance, and valuable and active interest in this work.

My great appreciation is expressed to the Dean of the College of Engineering ***Dr. Abd AL-Wahid K. Rajih*** and also to the head of Mechanical Engineering ***Dr. Adil A. AL-moosawy***.

My special thanks and deepest and warmest gratitude are due to my family with special gratitude to my wife for their kindness, love, support and encouragement during the period of preparing this work.

Furthermore, deepest thanks to my friends for their help to accomplish this study. Finally, I would like to express my deepest thanks and gratitude to all those who have helped me in one way or another in carrying out this research.

Sabah Aoada
2007

Abstract

A comprehensive mathematical model has been developed for the simulation of the behavior of a downward heat transport passive condensate pumping system. It has been assumed that saturation conditions prevail at all times in the liquid-vapor mixture of the working fluid inside the boiler.

A passive pumping heat pipe system has been analyzed for a various elevations, input powers, mass flow rate of water and working fluid.

The accumulator temperature was assumed near the prevailing surrounding temperature. During the pumping process, heat transport takes place due to evaporation and condensation of the working fluid. The condensate was pumped to the accumulator by virtue of a pressure difference between condenser and accumulator. Governing equations (mass conservation and energy conservation) to that model, the transient behavior of various system components are developed and solved.

A computer program was built to predict the numerical calculation of pressure and temperature of the boiler and the condenser. The computer also predict the circulated mass between the boiler and the accumulator. The exit water temperature and system efficiency are also predicted. The Rung-Kutta method was used to solve the governing equations.

The effects, on the behavior of the system, of the most important controlling thermodynamics properties of the working fluid, e.g., pressure, temperature, latent heat of evaporation, liquid density and specific heat have been tested and suggestions have been laid down for the selection of proper fluid for systems of various heights, circulating masses and input powers.

The calculated efficiency in the present work, as well as the available measured efficiencies from literature of this passive pumping system with the superior heat carrier (vapor) have been found to be more or at least equivalent to that of a conventional system (wick heat pipe).

It was observed in the present work, the temperatures of the boiler and the condenser increase when the applied load on the boiler increased. The efficiency of the system increases during increasing mass flow rates of cooling water, height of the accumulator and circulating mass between the boiler and the accumulator. Also three zones can be shown during the operating of the system are, no pumping zone, the transitional zone and the pumping zone. The results of R-11 when using (2000w) input power, height (15m) and mass flow rate for cooling water (0.015) kg/s. The temperature of boiler, condenser and efficiency are (90.78ºC,81.17ºC and η=89.3) respectively, the same conditions previous but using R-114 the results are (68.87ºC, 64.18ºC and η=64.4) respectively.

List of Contents

Nomenclature

The following symbols are used generally throughout the text. Other are defined as when used.

Symbol	***Description***	***Unit***
A_L	Area of liquid line	m^2
A_{vo}	Outer surface area of vapor line	m^2
c_p	Specific heat at constant pressure	J/kg.K
d_c	Coil diameter	m
D	Diameter of condenser shell	m
d_i	Inside diameter of pipe	m
d_o	Outside diameter of pipe	m
f	Fraction factor	_
G_b	Mass flow rate per unit area	kg/m^2. s
h	Enthalpy	J/kg
H	Total length of liquid line	m
k_g	Vapor thermal conductivity	W/m .K
k_L	Liquid thermal conductivity	W/m .K
L	Length between the boiler and the condenser	m
m	Mass	kg
$\dot{m}_b$	Vapor mass flow rate leaving the boiler	kg/s
$\dot{m}_c$	Liquid mass flow rate leaving the condenser	kg/s
$\dot{m}_{F.V}$	Liquid mass flow rate leaving or entering the float valve	kg/s
$\dot{m}_w$	Cooling water mass flow rate	kg/s
Nu	Nusselt number	_
Pr	Prandtle number	_
$\dot{Q}_b$	Input power for the boiler	W

$\dot{Q}_V$	Heat rate lost from the vapor	W
$\dot{Q}_L$	Heat rate lost from liquid line	W
Re	Reynolds number	_
t	Time	S
T	Temperature	K
T_∞	Ambient air temperature	K
T_{ec}	Outlet temperature of the cooling water to the condenser	K
T_{ic}	Inlet temperature of the cooling water to the condenser	K
T_w	Water temperature	K
t_T	Pumping period	S
t_{np}	No pumping zone time	S
t_{pz}	Pumping zone time	S
t_{tz}	Transitional zone time	S
u	Internal energy per unit mass	J/kg
U_o	Overall heat transfer coefficient based on outer area	W/m^2 .K
V	Volume	m^3

Greek Symbols

μ	Viscosity	$N.s/m^2$
ρ	Density	kg/m^3
$\Delta\theta$	Log mean temperature difference	K
ΔP_{bc}	Pressure drop along the vapor line	Pa
ΔL	Length of one cell	m

Subscripts

a	Refer to quantities related to accumulator
ao	Initial condition pertaining to accumulator
ae	Saturated equilibrium condition at the accumulator
bo	Initial condition pertaining to boiler
b	Refer to quantities related to condenser
c	For coil
co	Initial condition pertaining to condenser
ce	Saturated equilibrium condition at the condenser
cw	Condenser water
ec	Exit water temperature
f	Refer to saturated liquid properties
fg	Refer to the value of property in the vapor phase minus its value in the liquid phase
g	Refer to saturated vapor properties
ic	Inlet water temperature
L	For straight pipe
s	Surrounding
fF	Fluid inter the boiler via float valve

gb	Vapor in boiler
fb	Fluid in boiler

Introduction

1.1. General.

The term "heat pipe" is not only restricted the conventional heat pipes in which the condensate return is achieved by capillary forces which are established by the capillary wicks, but also used to describe all high thermal conductance devices in which the condensate return is achieved by other means, ***Dunn and Reay***, [1]. High effective thermal conductance comes from the fact that since the latent heat of evaporation is large, considerable quantities of heat can be transported with a very small temperature difference from end to end.

Recently, many ideas have been suggested to enhance cooling systems or computer processors aboard space shuttles, satellites, and even portable computers. One of the recent approaches involves cooling by integrating loop heat pipes. In general, loop heat pipes differ from conventional heat pipes Figure[1-1] found in [2] in the following manner: (1) LHP's a rearranged in a loop. (2) Wick complexity is only in the evaporator. (3) Vapor and liquid flow is in the same direction. (4) High capillary pumping and low flow impedance. Moreover, both types of heat pipes transfer heat efficiently with small temperature difference, include no mechanical parts, and use passive capillary pressure as the pumping force. Therefore, heat pipes can function in the presence of adverse gravity. Many devices have appeared recently trying to enhance heat flux removal. Recent electronic devices create huge heat fluxes that require more efficient heat removal systems. Different ideas have been used to develop such high performance cooling systems and devices. These devices are now used in aerospace applications and advanced electronic systems. Space applications require lightweight equipment. Therefore NASA is interested in such devices where no pump is needed and the system is self-circulating. Heat pipes' utilizing passive forces to circulate a working fluid in a loop system is one recent development. Researchers try to utilize the passive forces in the liquid such as

capillary effect, osmotic effect, viscosity effect, and expansion effect to create a self circulating system. The main idea of previous systems is to create a gradient of driving forces in the loop, forcing the working fluid to circulate in the loop. The LHP a device is able to transfer a large amount of heat with a small temperature difference due to the latent heat of evaporation. Also, it is important to distinguish between a loop heat pipe (LHP) and a capillary pumped loop (CLP). A schematic diagram with different components of a LHP is presented in Figure (1-2) while a CPL is presented in Figure (1-3) found in ***Hamdan et al,*** [3]. It is clear that a CPL and a LHP are similar in the components but differ in the arrangements. The major arrangement design difference is the position of the compensation chamber. In a LHP, the compensation chamber is directly attached to the evaporator while in a CPL the compensation chamber is connected to the evaporator through a piping system. This design difference results in a LHP being more robust and simpler to start. The preconditions required for CPL start-up is a major disadvantage that makes the LHP a good replacing and competing technology. The same advantage of a LHP over a CPL is considered as a disadvantage from a packaging point of view, since it adds some integration and packaging difficulties. In many cases and due to design limitations it is very difficult to have the compensation chamber directly connected to the evaporator. ***Nikitkin and Cullimore***, [4] discussed the advantages and disadvantages of the CPL and LHP in more detail. Figure (1-2) shows a schematic diagram of a LHP, while Figure (1-3) shows a schematic diagram of a CPL. The first appearance of the LHP was in the former Soviet Union in the early 1980s. On the other hand, the CPL appeared in the United State around the same period. The development of these devices have been encouraged by different applications such as cooling the high power electronics used in notepad computers and space shuttles. Also, with some modification and utilizing different working fluid, these deceives can be modified for cryogenic surgery applications. Many studies have appeared recently attempting to model and characterize loop heat pipes and capillary

pumped loop. Some of these studies have investigated the effect of different working fluids. Choosing the working fluid depends upon the application and the design limitations. ***Chandratilleke et al***, [5] investigated four different working fluids trying to develop loop heat pipes that can work in the cryogenic temperature range of 4 to77 K. Also, ***Chandratilleke et al***, [5] showed that loop heat pipes were able to transport at least 10 times the amount of heat as compared to a solid copper rod of the same size. A diameter optimization was presented by ***H_lke et al,*** [6] for a micro coherent porous silicon wick using water as the working fluid. ***H_lke et al,*** [6] showed that an effective way to increase the loop heat pipe's performance is by reducing the pressure drop in the evaporator. In order to create a fixed stable physical interface inside the capillary pumped loop, a conventional tube condenser was replaced by a porous wick as reported by ***Muraoka et al,*** [7]and [8]. It was found, that the existence of a porous wick inside the condenser could reduce or even eliminate the difficulties associated with the start-up procedure and the occurrence of the pressure oscillation during operation. ***Muraoka et al,*** [7] and [8] conducted an experimental and theoretical study as an extension of ***Schweickart et al***, [9]. ***Swanson and Herdt***, [10] reported a theoretical model for meniscus evaporation including Maragoni effect as well as London-Van der Waal dispersion forces. They used the 3-D Young Laplace equation to model the meniscus in a circular tube. ***Kaya and Hoang***, [11] used a primary and a secondary wick inside the evaporator to ensure that liquid stay in the wicks all the time. ***Figus et al***, [12] simulated numerically the flow in the evaporator of capillary pumped loop. Figus and his group found that capillary fingering may limit the operating range of the CPL. In that later study, Figus et al presented two models that gave similar results. They are a continuum (Darcy model) and a pore network model. As will be shown later, and as reported by ***Ku***, [13], many of the phenomena related to the LHP appear unusual, even for CPL experts. One such phenomenon is interfacial oscillation that has been studied by ***Kamotani,*** [14]. ***Kamotani,*** [14] reported that this behavior of the fluid depends

upon the critical temperature difference between the heater and the sidewall. It was observed that periods of strong and weak motion appear during one oscillation cycle. It is observed that very few theoretical and experimental LHP models are available in the literature. This is due to (1) the complexity of phase change, (2) the different phenomena related to LHP, and (3) the limited amount of data that has been published. Phase change occurs by different mechanisms depending on many factors such as the temperature difference between the fluid and the hot surface, surface structure, gravity, and fluid pressure. These factors are discussed in different places in the literature and will not be covered here [15]. Many different phenomena related to the LHPs which have appeared in experiments, still need more study and analysis. These phenomena are bubble formation in the compensation chamber, interface oscillation, and wick dry out. The first patent related to a LHP was issued in the United State of America to ***Maidanik et al***, [16] in 1985. The transient behavior of CPL has been discussed by different investigators such as ***LaClair and Mudawar***, [17]. A model of the steady state behavior of the LHP can be found in ***Kaya***, [18]. Kaya presents a mathematical steady state model for LHP, and including experimental validation.

Some application of very "Long Heat Pipe" (LHP) might involve the downward transfer of heat. If the vertical distance downward is more than a few centimeters, capillary wicks are no longer effective in the presence of gravity. Therefore, some sort of pumping must be required to force the condensate to the overhead boiler, ***Gari and Fathallah***, [19]. The driving force which pumps the working fluid from the condenser, located downward, towards the boiler, located above, arises from the pressure difference between the condenser vapor pressure and the accumulator vapor pressure. A direct lift of the working fluid (liquid) from the condenser to the boiler is not possible since the vapor pressure of the boiler is always higher than the vapor pressure of the condenser. Therefore, an accumulator is needed as an intermediate reservoir whose temperature, and hence its vapor pressure, should be kept as low as possible in comparison with the

condenser vapor pressure to ensure the necessary pressure difference between the condenser and the accumulator. The accumulator should be situated at a position (level) higher than the boiler position so that the accumulated working fluid can be returned passively, by gravity, to the boiler once the pumping time is over.

The presence of an accumulator makes the operation of the (LHP) system characterized by the condensate pumping and boiler charging processes.

During the pumping process, heat transport takes place due to evaporation and condensation of the working fluid. The condensate is pumped to the accumulator by virtue of the pressure difference between the condenser and the accumulator. The boiler and condenser pressures differ only because of the pressure drop due to the friction in the vapor line. Sub cooling the condensate to the surrounding temperature, T_s, occurs in the sub-cooler part of the condenser unit and in the liquid line joining the condenser and the accumulator. If sub cooling of the working fluid in the condenser and the liquid line is eliminated, the accumulator will heat up. This will eventually raise the pressure in the accumulator leading to a need for a larger boiler pressure to lift the condensate and therefore a higher temperature.

Note that as heat is delivered to the boiler, the working temperature it reaches will depend upon the actual temperature of the accumulator, this temperature which is an independent variable of the system; i.e. T_{ao} is a controlling parameter.

Pumping of the working fluid continues until a certain level is reached in the boiler, at which point a float-controlled boiler-accumulator equalization line opens and boiler charging starts.

During the boiler charging process, condensate pumping stops because the accumulator and boiler pressures are equalized. The boiler is charged with the working fluid (liquid phase) via a check valve from the accumulator by gravity. When the liquid in the boiler rises to a pre-determined level, the boiler-accumulator equalization line closes and the condensate pumping starts up again.

The working fluid in the LHP determines the range of the operating temperature. Table (1-1) lists some of the commonly used working fluids, their melting and boiling points at atmospheric pressure, and the operating temperature range. Depending on the operating temperature, LHPs are classified into four categories: Cryogenic (4-200K), low (200-550K), medium (550-750K), and high (750K and above) temperature ranges. Most LHP application falls in the low temperature range. The choice of working fluid must determine the account of the compatibility between the working fluid and the material of the LHP. Any chemical reaction between the working fluid and the material of the LHP creates non-condensable gas (NCG) in the system. The existence of (NCG) degenerates the performance of a LHP. Information concerning compatibility of metals with working fluids can be found in ***Chuang***, [20].

1.2. The aim of the present work.

In the present work, a mathematical model will be developed to study the behavior of the system during the pumping time. In this model, the boiler is assumed to contain a mixture of the liquid and vapor at all times. Heat losses and minor temperature drops of the vapor in the vapor line are accounted for. The heat and mass balances equations are solved using the "Runge-Kutta" method to predict the temperature variations of boiler and condenser. The variation of mass within the boiler of accumulator are also predicted. It must be mentioned that the mass within the condenser is assumed to be constant.

1.3. Book layout.

This thesis is organized in five chapters:

Chapter One.

Introduces and explains briefly the problem of the study, the aim of the study, (using and analysis of the heat pipe).

Chapter Two.

Contains a brief review of the previous studies on the subject under consideration.

Chapter Three.

Presents the formulation of the mathematical model and computer program.

Chapter Four.

Presents and discusses the results and the effect of some parameters, such as height, mass flow rate of water, and working fluid on the LHP performance.

Chapter Five.

Gives the conclusions drawn from this study and suggestions for further works.

Table (1-1): Operating temperature range of various working fluids, [20].

Working fluid	Melting point, K At 1 atm	Boiling point, K At 1 atm	Operating temperature range, K	Classified Temperature application
Helium	1.0	4.2	2-4	Cryogenic
Hydrogen	13.8	20.4	14-31	Cryogenic
Neon	24.4	27.1	27-37	Cryogenic
Nitrogen	63.1	77.4	70-103	Cryogenic
Argon	83.9	87.3	84-116	Cryogenic
Oxygen	54.7	90.2	73-119	Cryogenic
Krypton	115.8	119.7	116-160	Cryogenic
Ammonia	195.5	239.9	213-373	Low temperature
Pentane	143.1	309.2	253-293	Low temperature
Freon113	236.5	320.8	263-373	Low temperature
Acetone	180.0	329.4	273-393	Low temperature
Water	273.1	373.1	303-473	Low temperature
Mercury	234.2	630.1	523-923	Medium temperature
Sulphur	385.9	717.8	530-947	Medium temperature
Sodium	371.0	1151	873-1473	High temperature
Lithium	453.7	1615	1273-2073	High temperature
Silver	1234	2385	2073-2573	High temperature

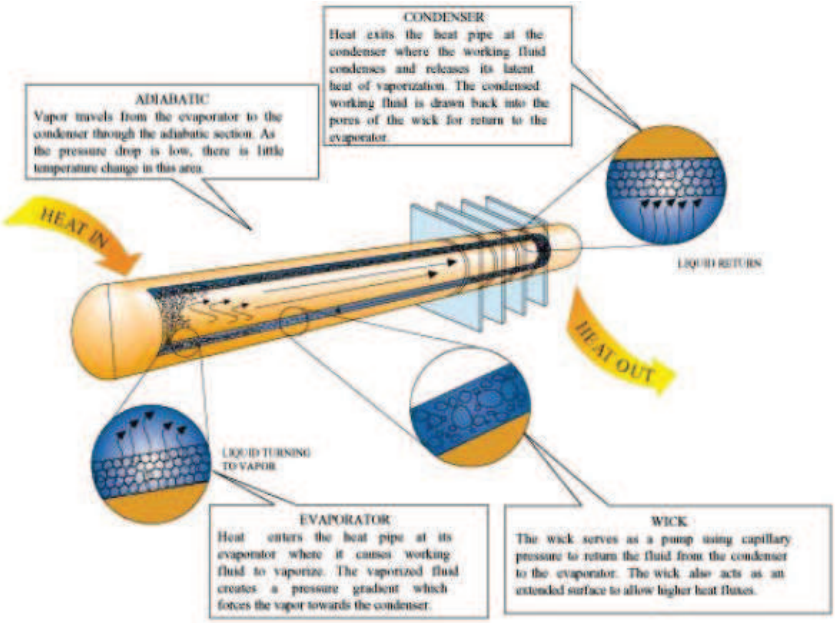

Figure (1-1): Conventional heat pipe. [2]

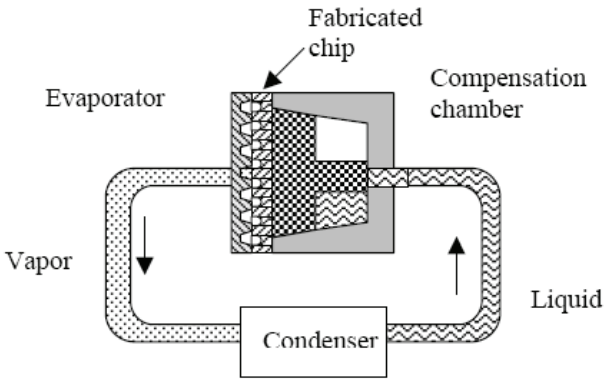

Figure (1-2): Loop heat pipe, LHP, with major parts. [3]

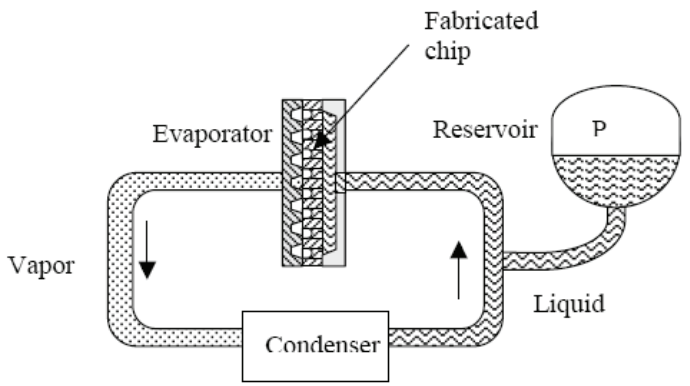

Figure (1-3): Capillary pumped loop, CPL, with major parts. [3]

Literature Review

2.1. Historical development.

The loop heat pipe is a particular kind of heat pipe, the history of heat pipes must be discussed first. The uniqueness of a heat pipe is the existence of a wick structure in the system to transport heat against gravity by an evaporation-condensation cycle. However, many heat pipe applications do not need to rely on this feature, and the Perkins Tube, which was invented decades before the heat pipe, is basically a form of thermosyphon that is still being used today. Therefore, the Perkins tube became an essential part of the history of the heat pipe.

2.1.1 The Perkins tube (Thermosyphon).

The predecessor of the heat pipe, the Perkins tube, was introduced by the Perkins family from the mid-nineteenth to the twentieth century through a series of patents in the United Kingdom. Most of the Perkins tubes were wickless gravity-assisted thermosyphons, in which heat transfer was achieved by evaporation. A Thermosyphon refers to a heat transfer device in which the working fluid is circulated by the density difference between a cold temperature and a hot temperature fluid or between vapor and liquid. The design of the Perkins tube, which is closest to the present heat pipe, was described in a patent by Jacob Perkins can be found in ***Chuang***, [20]. A schematic drawing of the Perkins tube is shown in Fig. (2-1). This design was a closed tube containing a small quantity of water operating in either a single- or two-phase cycle to transfer heat from a furnace to a boiler. The water in the closed loop is boiled into steam when passing through the furnace, and flows to the boiler. In the boiler, the heat is rejected and the steam is condensed back to water. Because there is no wick structure in the system, it can operate efficiently only when the boiler was placed above the furnace.

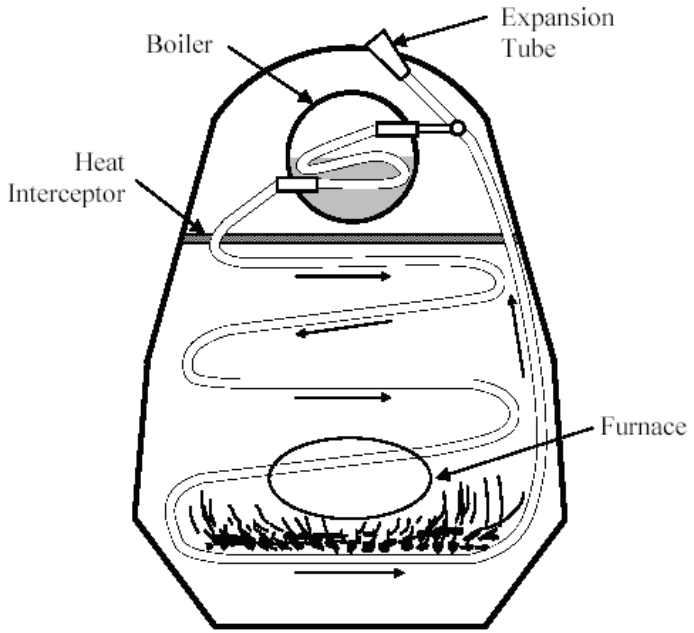

Fig. (2-1): A schematic diagram of Perkins Tube, [20].

In the development of the Perkins tube, the most interesting improvements were made by L. P. Perkins and W. E. Buck can be found in ***Chuang***, [20]. Their work focused on the study of the fluid inventory. While water was the only specific working fluid, they tested the use of anti-freeze type fluids, and fluids having a higher boiling temperature than water at atmospheric pressure.

2.1.2 The heat pipe.

The heat pipe was first conceived by R. S. Gaugler can be found in ***Chuang***, [20] of the General Motors Corporation in the U.S. Patent No. 2350348. Gaugler, who was working on refrigeration problems at that time, envisioned a device that would evaporate a liquid at a point above the place where condensation would occur, without requiring any additional work to move the

liquid to the higher elevation. His device consisted of a closed tube in which the liquid would absorb heat at one location causing the liquid to evaporate. The vapor would then travel down the length of the tube where it would condense and release its latent heat. It would then travel back up the tube by capillary pressure to start the process over. In order to move the liquid back up to a higher point, Gaugler suggested the use of a capillary structure consisting of a sintered iron wick. In 1962, Trefethen resurrected the idea of a heat pipe in connection with the space program. The heat pipe concept received relatively little attention, until Grover et al., published the results of an independent investigation and first applied the term heat pipe to describe a "synergistic engineering structure which is equivalent to a material having a thermal conductivity greatly exceeding that of any know metal". Grover built several prototype heat pipes, the first of which used water as a working fluid and was soon followed by a sodium heat pipe which operated at 1100 K. Since that time, heat pipes have been employed in numerous applications ranging from temperature control of the permafrost layer under the Alaska pipeline to the thermal control of optical surfaces in spacecraft. The first commercial organization to work on heat pipes was RCA. They made heat pipes using glass, copper, nickel stainless steel, molybdenum and TZM molybdenum as wall materials. Working fluids included water, cesium, sodium, lithium, and bismuth. Maximum operating temperatures of (1650°C) had been achieved. The early development of terrestrial applications of heat pipes proceeded at a slow pace. Since heat pipes can operate in micro-gravitational fields due to capillary action without any external force field or pump, most early efforts were directed toward space applications. However, due to the high cost of energy, especially in Japan and Europe, the industrial community began to appreciate the significance of heat pipes and thermosyphons in energy savings as well as design improvements in various applications. A heat pipe typically consists of a sealed container lined with a wicking material. The container is evacuated and back filled with just enough liquid to fully saturate the wick.

Because heat pipes operate on a closed two-phase cycle and only pure liquid and vapor are present within the container, the working fluid remains at saturation conditions as long as the operating temperature is between the triple point and the critical state. As illustrated in Fig. (2-2), a heat pipe consists of three distinct regions: an evaporator, a condenser, and an adiabatic region.

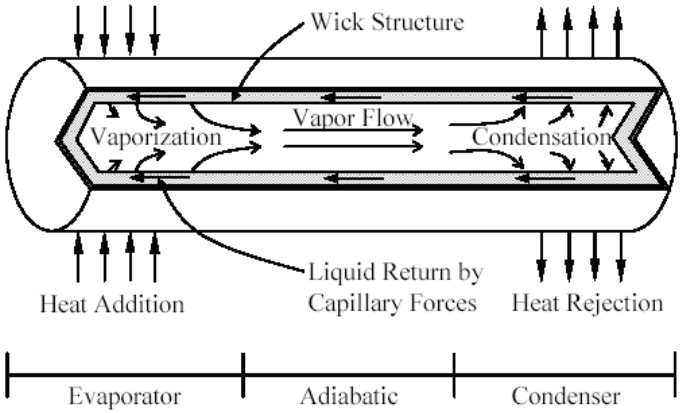

Fig. (2-2): A schematic diagram of a conventional heat pipe, [20].

When heat is added to the evaporator region of the container, the working fluid presented in the wicking structure is heated until it vaporizes. The high temperature and corresponding high pressure in this region cause the vapor to flow to the condenser region, where the vapor condenses and gives up its latent heat of vaporization. The capillary forces existing in the wicking structure then pump the liquid back to the evaporator.

2.2 The capillary pump loop

The capillary pumped loop (CPL) is very similar to the loop heat pipe. The CPL was invented by F. J. Stenger 1966 of NASA Lewis Research Center, but serious development did not begin until the late 1970s. In 1982, an aluminum-ammonia CPL with the capability of transporting 6.4 kW (15 W/cm^2) over 10

meters was manufactured by OAO Corporation (NASA Goddard's CPL-1). In 1985 and 986, the first flight experiments of CPL technology were successfully tested [Ku et al., 1986]. In the 1990s, extensive ground testing had been performed, and the potential of the CPL as a reliable and versatile thermal transport system for space applications was demonstrated. Fig. (2-3) shows a drawing of a typical capillary pumped loop.

The main difference between a CPL and a LHP is the location of the reservoir (a.k.a. compensation chamber). In a CPL, vapor generated in the evaporator flows to the condenser, where the vapor is condensed back to liquid, and liquid exits the condenser with a small amount of sub cooling. The liquid flows back to the evaporator through the liquid line and the bayonet. In the evaporator core, a secondary wick is usually used to prevent any bubbles from blocking the liquid path to the primary wick. The liquid then flows radially to the outer surface of the primary wick to complete the cycle. The reservoir in a CPL is physically isolated from the loop. It is connected to the liquid line by a reservoir line to store excess liquid in the system. The primary wick in the CPL is usually made of polyethylene to minimize the heat conducted through the primary wick and vaporize the liquid in the evaporator core. The pore size of a polyethylene wick is around 15 μm. Due to these construction differences, the behavior between a CPL and a LHP differs in many ways. A major difference is the start-up characteristics. A CPL requires pre-conditioning of the loop, usually by heating the reservoir, in order to ensure that the wick is fully wetted. One advantage of CPL is that the operating temperature can be controlled precisely by the reservoir set point temperature regardless of changes in the heat load or sink temperature. CPLs and LHPs have their own advantages and disadvantages depending on the application. A detailed overview of CPLs can be found in ***Chuang***, [20].

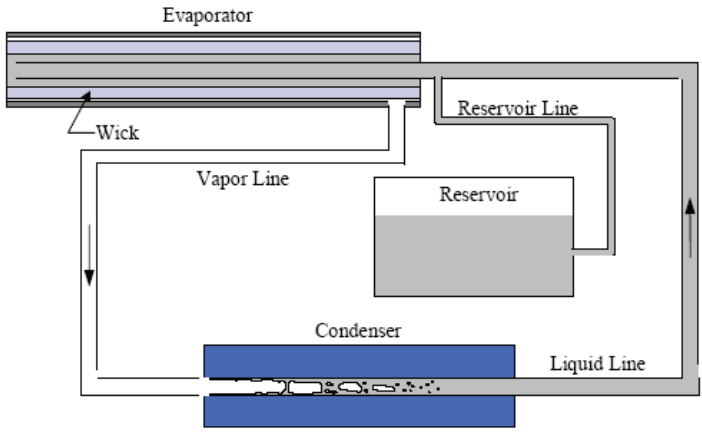

Fig. (2-3): A schematic diagram of a capillary pumped loop, [20].

2.3. The loop heat pipe.

Generally speaking, heat pipes are excellent heat transfer devices. Advantages of heat pipes include a very high thermal conductance, no pumping power requirements, no moving parts, and relatively low pressure drops produced by the system. But serious constraints on conventional heat pipes are the reduction of transport capabilities over long distances and when it was operated against gravity, which means the condenser is located below the evaporator.

Loop heat pipes are developed to provide the solution to this problem. Loop heat pipes (LHPs) were invented at the Urals Technical University in Russia in 1971 and patented in the USA by Maidanik et al can be found in ***Chuang***, [20]. LHPs were used in space for thermal management purposes, especially on satellites. After successfully demonstrating the heat transport capability and reliability in space applications, LHPs started gaining worldwide attention in the late 1980s. Since then, numerous studies focusing on improving the efficiency of the system and understanding its operating characteristics have been conducted. The LHP is known for its high pumping capability and robust operation because it uses fine-

pored metal wicks and the integral evaporator/reservoir design. It is the baseline design for thermal control of several spacecraft and commercial satellites.

2.4. Passive heat transport system.

Passive downward heat transport system are often favored because of their intrinsic reliability, and simplicity, and because they reduce costs and require limited maintenance; for, once installed, they can be conveniently forgotten .The renewed interest towards the application of passive technologies is not only directed to the arrangement of living spaces (as it was already done in ancient houses), but also for the production of hot water, usually through thermosyphon loops directly linked to the solar heat collectors ***Mertol et.al***, [21].

A reliable passive system for downward heat transport allows the choice of a batter place for the hot water reservoir, letting the collectors in their optimum place (e.g. on the roof). There are many other circumstances in which a passive system would be highly desirable, e.g., places where no electrical or mechanical energy is available for running the pumps, remote regions or those where technical assistance is scarce, projects for the heating the soil up to a certain depth (seasonal storage of solar energy) ***Brun***, [22], or for the heating of swimming pools.

Condensate pumping can be done by mechanical pumps, as it is customary in the steam and chemical plant applications. In heat pipe work however, due to the extreme sensitivity of the process to the presence of non-condensable gases, it would be preferable to avoid any design that would endanger the hermetically sealed environment of the heat pipe. A fully contained pumping system that can be passively operated is, therefore, preferable to mechanical pumps.

2.4.1. Passive downward heat transport system.

Many proposals have been made in recent years for systems involving passive downward heat transport. Most of them are based on the evaporation /condensation steps, and a comprehensive review has recently been made, [23].

All these devices involve different types of heat pipes. For returning the condensate to a higher position alternatively, several passive condensate pumping schemes have been designed and tested by various investigators: heat source produces a kind of gas lift effect, or some mechanical energy produced inside the system or the pressure fluctuations in discontinuous systems are exploited, or, again, a semi-permeable membrane is introduced to exploit an osmotic pressure. Other systems, [24], are based on the increase of volume of liquids when the temperature is raised, or on the vapor pressure generated by a third fluid. The most familiar scheme is that in which the condensate is pumped to the accumulator by virtue of the pressure difference between the condenser and the accumulator.

Neepers and Hedstorm, [25], constructed and tested two types of self-pumping vapor systems for hybrid space heating using Refrigerant R-11as a working fluid. The first type consists of a single accumulator, check valve, collector (boiler), a condenser and a solenoid valve.

The operation of this system required external cooling of the accumulator and lifted the liquid 5.18m (17 ft). The second type consisted of two insulated accumulators with a float valve in the lower accumulator. The operation showed a liquid lift of 4.57m (15 ft) and a cycle time that was longer than the cycle time in the first system .No modeling or simulations were reported.

Beni and Friesen, [26], successfully constructed and tested a passive downward heat transport system using R-114.Although the actual vertical distance between the heat source and heat sink was 1m, the authors claim that by increasing (T) between the heat source and heat sink to 10 ºC, with minor adjustments in the spring loaded check valve, the vertical distance can reach up to 15m .No analytical solution or system modeling was provided.

Gari et al, [27] developed a simple one-dimensional steady state model to predict the performance of a long heat pipe passive condensate pumping system.

The system consisted of a boiler, a single accumulator, a condenser, and two checks valves. As illustrated in Fig. (2-4).

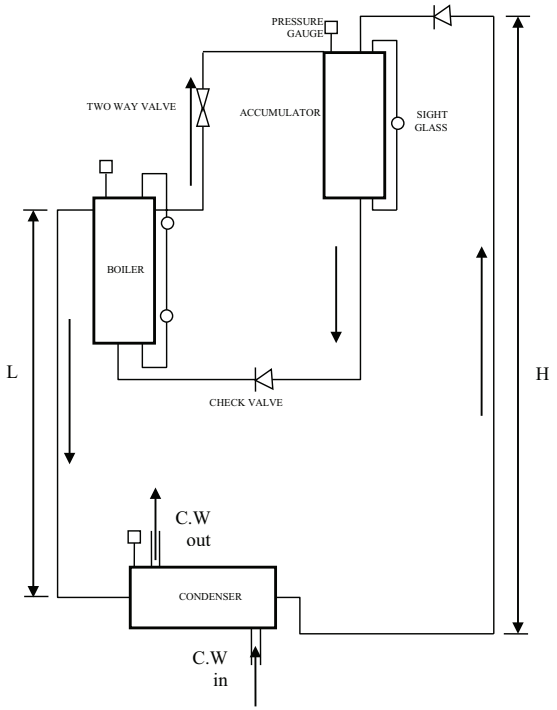

Fig. (2-4): A schematic diagram of passive heat transport system.

A comparison of the in house experimental results with the model predictions indicated that the unsteady effects resulting from the changes in boiler and accumulator stored masses and energies must be accounted for. In a subsequent paper, ***Gari et.al***, [28], they developed and solved the governing equations that model the transient behavior of the various components of the same system of their previous paper.

The most relevant literature sight can be summarized as below:

Chuang, [20]

Presented a thermodynamic mathematical analysis of three different heat pipe system.

1. Thermosyphone. 2. Conventional heat pipe. 3. Capillary pumped loop.

4. Loop heat pipe.

Mertol et al, [21]

Gave a thermodynamic description and analysis of a loop heat pipe linked to a solar heat collectors.

Neepers and Hedstrom, [25**]**

Constructed and studied experimentally two types of heat pipes using Refrigerant R-11 as the working fluid. In the first type lifted the liquid 5.18m and second type lifted the liquid 4.57m. No modeling or simulations were reported

Beni and Friesen , [26]

Tested experimentally a passive downward heat transport system using R-114 as a working fluid. They claimed that by increasing the temperature difference between the source and sink to 10ºC with miner adjustment to spring loaded check value a height of 15 m can be achieved.

Gari et al (second report), [27]

Developed a simple one-dimensional steady state model to predict the performance of a long heat pipe passive condensate pumping system.

Gari et al (third report), [28]

They developed and solved the governing equations that model the transient behavior of the various components of the same system of their previous paper.

In the present work

The present work devoted to the mathematical thermodynamic analysis of each component of the loop heat pipe. The mass and the energy equations for each component are solved numerically by using runge-kutta method. The

pressure drop in the vapor line and through each of the boiler and condenser is predict. The efficiency of the loop heat pipe system is also predicted.

Mathematical analysis

and

Computer program

3.1. Introduction.

Figure (3-1) shows a schematic drawing of a long heat pipe passive condensate pumping system. It consists of a boiler, a condenser, an accumulator, two check valves, float valve and a working fluid.

The operation of the system can be summarized, the working fluid inside the boiler is saturated applied heat load on the boiler, the heat load can be provided by any source such as electrical source, after supplied the heat load the working fluid starts to raise the temperature at a constant pressure to evaporate the liquid in the boiler. After reaches the target pressure the vapor flow out the boiler to the vapor line, the vapor line in (P_b and T_b), in the vapor line can be throttling the vapor from, P_b to P_c, the vapor enters the condenser the vapor condensate at (P_c and T_c). The heat is delivered to the cooling water at, T_c. Leaving the liquid the condenser to the liquid line in the liquid line the sub cooling occurs finally the liquid enters the accumulator at a saturation temperature. After that the accumulator charged the liquid to the boiler when the level liquid decreases in the boiler. In the present work focuses on the pumping process.

3.2. Assumptions.

In developing the mathematical model and solving the governing equations for the system, the following assumptions are made:

I. Saturation conditions prevail in the boiler.

II. No accumulation of working fluid in the condenser.

III. The temperature of the accumulator T_a has a predetermined value approximately equal to the surrounding temperature T_s.

V. Instant charging of the boiler.

3.3. Thermodynamic cycle of the system.

Thermodynamic processes involved in the operation of the LHP passive pumping system are depicted in the (h-s) and (T-s) diagram of Fig. (3-2). Process (1-2) is a constant pressure heat addition in the boiler. Process (2-3) is a constant enthalpy throttling from the boiler pressure, (P_b), to the condenser pressure, (P_c). The boiler contains saturated liquid at state (1) and saturated vapor at state (2). In the condenser, the vapor is condensed at a pressure (P_c) and temperature (T_c). Heat is delivered to the cooling water (storage) at temperature (T_c). Sub cooling the working fluid a surrounding temperature (T_s) occurs in the liquid line joining the condenser and the accumulator. Any attempt to accomplish the entire cooling process of working fluid to (T_s) in the condenser does not represents the physical problem. If sub cooling of the working fluid in the condenser-accumulator line is eliminated, the accumulator will heat up. This will cripple the operation of the system. Sub cooling then brings the fluid to state (5) at (P_c) and (T_s). Pumping to the accumulator is achieved by maintaining a pressure difference (P_c-P_a) between the condenser and the accumulator. The sub cooling temperature (T_s) may be chosen to satisfy $u_{fa}(T_a)=h_{fs}(T_s)$ from ***Gari and Fathallah,*** [19], where (u_{fa}) and (h_{fs}) are the saturated liquid internal energy at (T_a) and the saturated liquid enthalpy at (T_s), respectively. If the above condition is not fulfilled, the accumulator temperature will change according to the accumulator's energy

balance. Saturated liquid at state (6) will be stored in the accumulator; it will be delivered to the boiler when the boiler-accumulator pressure equalization valve is opened. State (7) results from the mixing process between the boiler charge at state (1) and the accumulator charge at state (6). The boiler charge is then transiently heat back to state (1).

3.4. Pumping time

Qualitative Analysis

The operation of the system during the pumping time is characterized by the existence of three distinguished zones, namely:

1. No pumping zone, which is characterized by a continual increase in the boiler pressure (and its saturation temperature) towards the target pressure ($P_s=P_a+\rho_s gH$), to provide the necessary force needed to lift the condensate to the accumulator. The temperature of the stagnant working fluid (liquid) inside the coil is affected by the temperature of the cooling water through heat transfer by conduction across the coil wall, and the condenser pressure follows the boiler pressure ,i.e. $P_{b=}P_c$. The accumulator isn't affected yet, neither temperature wise nor pressure wise. Its temperature is the same as its initial value (T_{ao}) and its pressure is equal to its saturation pressure at T_{ao}.
2. Transitional zone, which is marked by the beginning of downward heat transport carried by the vapor flow from the boiler to the condenser where it is condensed and returned to the accumulator by virtue of pressure difference between the condenser and the accumulator. The pressure inside the condenser remains nearly constant at (P_s) and it controls the pressure inside the accumulator which will be equal to ($P_a=P_s-\rho_s gH$), while the temperature of the two phase region inside the coil is less than the corresponding saturation temperature for the prevailing pressure (P_s). The temperature of the accumulator remains nearly constant.
3. Pumping zone, which starts when the temperature of the two-phase region inside the condenser reaches the corresponding saturation value at the

prevailing pressure. As regards the accumulator, the temperature of the working fluid (liquid) is still increasing at an even slower rate since the mass in the accumulator is increasing. The accumulator pressure, however, is higher than the saturation pressure at the prevailing temperature and is equal to (P_{ce}-ρ_sgH).

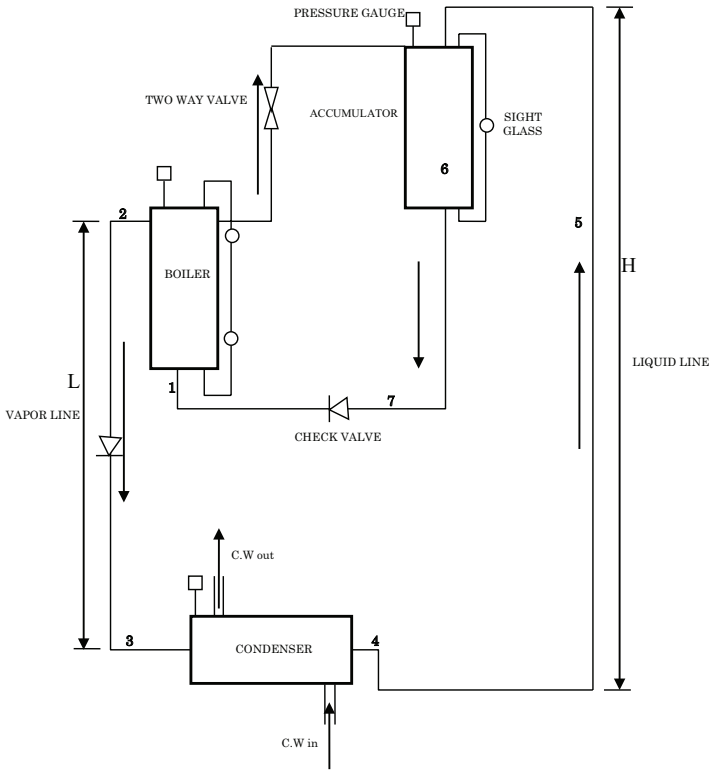

Fig. (3-1): Schematic Diagram of the heat pipe pumping system.[19]

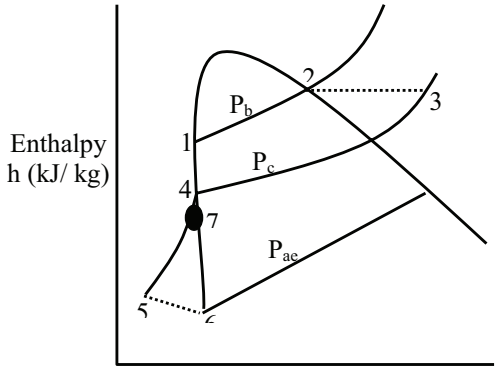

Entropy s (kJ/kg K)

Fig.(A), [19]

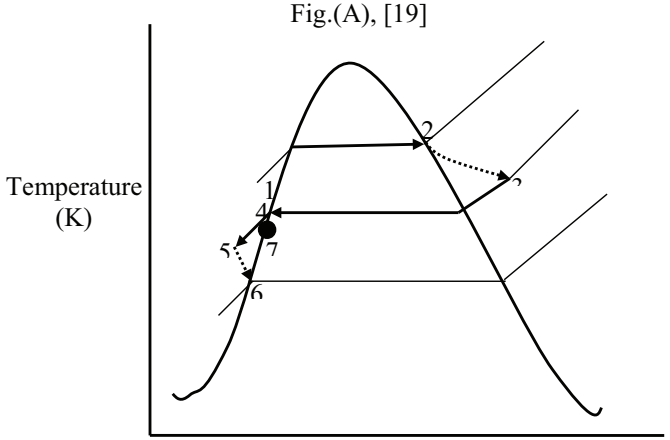

Entropy s (kJ/kg K)

Fig.(B)

Fig. (3-2). Enthalpy-entropy and temperature-entropy diagrams for the cycle of the working fluid

3.4.1. Boiler.

Assuming $\dot{m}_b$ a mass of rate leaves the boiler for the condenser, $\dot{m}_{F.v}$ leaves the accumulator for the boiler via the check valve and applying mass conservation for the boiler one get:

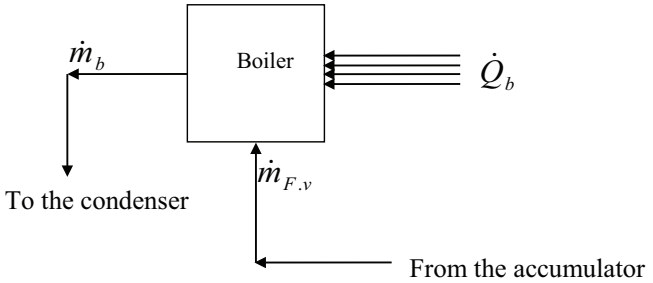

$$\frac{dm_b}{dt} = \dot{m}_{F.v} - \dot{m}_b \qquad \ldots(3.1)$$

Where $\frac{dm_b}{dt}$, rate of mass change within the boiler.

$\dot{m}_{F.v}$, is the mass flow rate of working liquid from the float valve into the boiler ,and can be calculated as follows:

$\dot{m}_b \Delta t = \rho_{fb} A_b \Delta L_b$, therefore, $\frac{\Delta L}{\Delta t} = \frac{\dot{m}_b}{\rho_{fb} A_b}$,

Similarly, $\frac{-\Delta L_F}{\Delta t} = \frac{\Delta L_b}{\Delta t} = \frac{\dot{m}_{F.v}}{\rho_{fF} \Delta A_f}$

Therefore, $\dot{m}_{F.v} = \left(\frac{\rho_{fF}}{\rho_{fb}}\right)\left(\frac{\Delta A_f}{A_b}\right)\dot{m}_b$, since $\rho_{fF} \approx \rho_{fb}$,

Hence, $\dot{m}_{F.v} = \left(\frac{\Delta A_f}{A_b}\right)\dot{m}_b$

Now applying conservation of energy to get, for boiler

$$\frac{dU}{dt} = \dot{Q}_b - \dot{m}_b h_{gb} \quad \ldots (3.2)$$

Where

$$U = m_b u_{fb} \quad \ldots (3.3)$$

Differentiating the above equation (3.3) with respect to time yields:

$$\frac{dU}{dt} = m_b \frac{du_{fb}}{dt} + u_{fb} \frac{dm_b}{dt} \quad \ldots (3.4)$$

Substituting for $\left(\frac{dU}{dt} \right)$ from Eq. (3.2) into Eq. (3.4) to get:

$$\dot{Q}_b - \dot{m}_b h_{gb} = m_b \frac{du_{fb}}{dt} + u_{fb} \frac{dm_b}{dt} \quad \ldots (3.5)$$

Substituting for $\left(\frac{dm_b}{dt} \right)$ from Eq. (3.1) into Eq. (3.5) to get:

$$\dot{Q}_b - \dot{m}_b h_{gb} = m_b \frac{du_{fb}}{dt} + u_{fb} (\dot{m}_{F.v} - \dot{m}_b) \quad \ldots (3.6)$$

Noting that $\frac{du_{fb}}{dt} = \frac{du_{fb}}{dT_b} \frac{dT_b}{dt}$ and neglecting the term containing $\dot{m}_{F.v}$

Eq. (3.6) becomes,

$$\frac{dT_b}{dt} = \left[m_b \left(\frac{du_{fb}}{dT_b} \right) \right]^{-1} \left[\dot{Q}_b - \dot{m}_b (h_{gb} - u_{fb}) \right] \quad \ldots (3.7)$$

Equations (3.1) and (3.7) are solved by the fourth order Runge-Kutta method for the total mass in the boiler and boiler temperature with the given initial values for (m_b and T_b). The various thermodynamic parameters are evaluated see appendix (A).

3.4.2. Vapor Line.

Saturated vapor, from the boiler, enters the vapor line joining the condenser and the boiler at temperature, T_b and saturation pressure.

The heat rate lost from the vapor line to air,

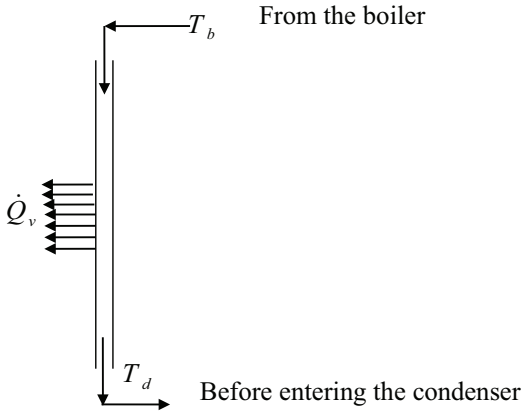

$$\dot{Q}_v = \dot{m}_b C_p (T_b - T_d) \quad \text{… (3.8)}$$

where, T_d ,the temperature enter the condenser

Also

$$\dot{Q}_v = U_o A_{vo} \Delta\theta_m \quad \text{… (3.9)}$$

Therefore

$$U_o A_{vo} \Delta\theta_m = \dot{m}_b C_p (T_b - T_d) \quad \text{… (3.10)}$$

Where,

$$\Delta\theta_m = \left[\frac{(T_b - T_\infty) - (T_d - T_\infty)}{\ln\left(\frac{T_b - T_\infty}{T_d - T_\infty} \right)} \right] = \left[\frac{T_b - T_d}{\ln\left(\frac{T_b - T_\infty}{T_d - T_\infty} \right)} \right] \quad \text{… (3.11)}$$

Then,

$$T_d = T_\infty + (T_b - T_\infty)\exp\left(\frac{-U_o A_{wo}}{\dot{m}_b C_p}\right) \quad \ldots (3.12)$$

Also can be calculated the water temperature exit from the condenser,

$$T_{ec} = T_c - (T_c - T_{ic})\exp\left(\frac{-U_o A_{wo}}{\dot{m}_w C_w}\right) \quad \ldots (3.13)$$

Since the prevailing mode of flow for vapor in the vapor line is turbulent, then,

$$h_i = 0.023\,\mathrm{Re}^{0.8}\,\mathrm{Pr}^{0.4}\left(\frac{k_g}{d_i}\right) \quad \ldots (3.14)$$

Also

$$h_o = 1.05\left(\frac{(T_b - T_\infty)}{d_o}\right)^{0.25} \quad \ldots (3.15)$$

Neglecting wall resistance and fouling, the overall heat transfer coefficient for the vapor line becomes,

$$U_o = \frac{1}{\left[\frac{1}{h_o} + \frac{d_o}{d_i}\left(\frac{1}{h_i}\right)\right]} \quad \ldots (3.16)$$

3.4.3. Condenser.

Assuming a mass of rate $\dot{m}_b$ leaves the boiler for the condenser, and $\dot{m}_c$ leaves the condenser for the accumulator, and applying mass conservation for the condenser one get:

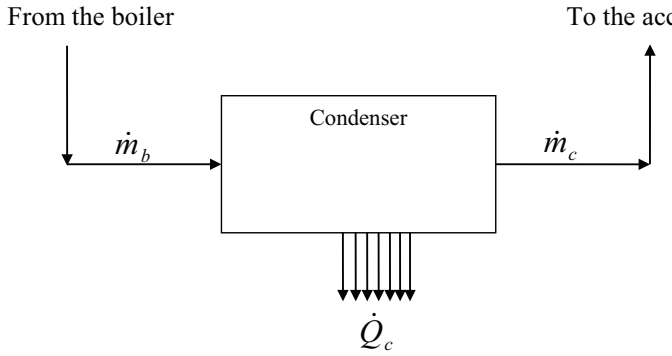

$$\frac{dm_c}{dt} = \dot{m}_b - \dot{m}_c \quad \text{… (3.17)}$$

Where, $\frac{dm_c}{dt}$ rate of mass change within condenser

Now applying conservation of energy to get,

$$\frac{dU}{dt} = -\dot{Q}_c - \dot{m}_c h_{fc} + \dot{m}_b h_{gb} \quad \text{… (3.18)}$$

Where, $\dot{Q}_c = \dot{m}_w C_w (T_{ec} - T_{ic})$

Where, $\dot{m}_w$, mass flow rate of cooling water.

Where, C_w, specific heat of cooling water.

Where, T_{ec}, temperature of water exit the condenser and, T_{ic}, temperature of water enters the condenser.

Where

$$U = m_c u_{fc} \quad \text{… (3.19)}$$

Differentiating the above equation (3.19) with respect to time yields

$$\frac{dU}{dt} = m_c \frac{du_{fc}}{dt} + u_{fc} \frac{dm_c}{dt} \quad \text{… (3.20)}$$

Substituting for $\left(\frac{dU}{dt}\right)$ from Eq. (3.18) into Eq. (3.20) to get:

$$m_c \frac{du_{fc}}{dt} + u_{fc} \frac{dm_c}{dt} = -\dot{Q}_c - \dot{m}_c h_{fc} + \dot{m}_b h_{gb} \quad \ldots (3.21)$$

Substituting for $\left(\frac{dm_c}{dt}\right)$ from Eq. (3.17) into Eq. (3.21) to get:

$$m_c \frac{du_{fc}}{dt} + u_{fc}\left(\dot{m}_b - \dot{m}_c\right) = -\dot{Q}_c - \dot{m}_c h_{fc} + m_b h_{gb} \quad \ldots (3.22)$$

Noting that $\frac{du_{fc}}{dt} = \frac{du_{fc}}{dT_c}\frac{dT_c}{dt}$ Eq. (3.22) becomes,

$$\frac{dT_c}{dt} = \left[m_c\left(\frac{du_{fc}}{dT_c}\right)\right]^{-1}\left[-\dot{Q}_c - \dot{m}_c\left(h_{fc} - u_{fc}\right) - \dot{m}_b\left(u_{fc} - u_{gb}\right)\right] \quad \ldots (3.23)$$

Equations (3.17) and (3.23) can be solved numerically by the fourth order Runge-Kutta method for the mass in the condenser and condenser temperature with the given initial values for m_c and T_c.

$\dot{m}_b$, is calculated from a consideration of the pressure drop along the vapor line as follows, from [19].

$$\Delta P_{bc} = P_b - P_c \quad \ldots (3.24)$$

Also

$$\Delta P_{bc} = f\left(\frac{L}{d_i}\right)\left(\frac{G_b^2}{2\rho_{gb}}\right) \quad \ldots (3.25)$$

Where

$$G_b = \frac{\dot{m}_b}{A_i} \quad \ldots (3.26)$$

And since the prevailing mode of flow in the vapor line is turbulent then,

$$f = 0.184\,\mathrm{Re}^{-0.2} \quad \ldots (3.27)$$

And

$$\mathrm{Re} = \frac{\dot{m}_b d_i}{A_i \mu_{gb}} = \frac{4\dot{m}_b}{\pi\, d_i \mu_{gb}} \quad \ldots (3.28)$$

Substituting Eqs. (3.26), (3.27) and (3.28) into Eq. (3.25) and simplifying to get,

$$\Delta P_{bc} = 0.092\left(\frac{\dot{m}_b}{A_i}\right)^{1.8}\left(\frac{\mu_{gb}^{0.2}}{\rho_{gb}}\right)\left(\frac{L}{d_i^{1.2}}\right) \quad \ldots (3.29)$$

And

$$\dot{m}_b = \left\{\left(\frac{1}{0.092}\right)\left(\frac{\rho_{gb} d_i^{1.2}}{\mu_{gb}^{0.2} L}\right)\Delta P_{bc}\right\}^{\frac{1}{1.8}} A_i \quad \ldots (3.30)$$

3.4.4. Liquid Line.

The liquid leaves the condenser is saturated liquid, the liquid line is not insulated therefore the liquid is lost some of the heat to the surrounding, therefore can be occurs sub cooling in the liquid line.

From continuity equation,

$$V_L = \frac{\dot{m}_b}{\rho_f A_i} \quad \ldots (3.31)$$

The heat lost from the liquid is given by:

$$\dot{Q}_L = U_L A_L \Delta T \quad \ldots (3.32)$$

Where,

$$\Delta T = T_L - T_\infty \quad \ldots (3.33)$$

And

$$A_L = \pi\, d_o H \quad \ldots (3.34)$$

And, U_L is calculated as follows:

For turbulent flow,

$$h_i = 0.023 \mathrm{Re}^{0.8} \mathrm{Pr}^{0.4} \left(\frac{k_L}{d_i} \right) \quad \ldots (3.35)$$

While for laminar flow,

$$h_i = 4.36 \left(\frac{k_L}{d_i} \right) \quad \ldots (3.36)$$

Also, for natural convection from long vertical pipes to air, Kern [29] recommends:

$$h_o = 1.050224 \left(\frac{(T_L - T_\infty)}{d_o} \right)^{0.25} \quad \ldots (3.37)$$

Neglecting wall resistance, the overall heat transfer coefficient for the vapor line becomes,

$$U_o = \frac{1}{\left[\frac{1}{h_o} + \frac{d_o}{d_i} \left(\frac{1}{h_i} \right) \right]} \quad \ldots (3.38)$$

And since the outside resistance is the controlling resistance then,

$U_o \cong h_o$

3.4.5 Accumulator.

Considering the liquid phase only, the conservation of mass for the accumulator becomes:

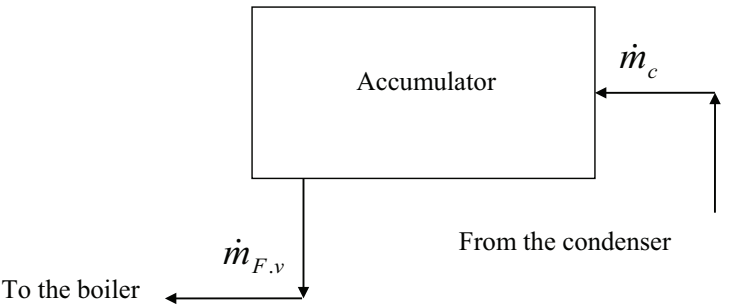

$$\frac{dm_a}{dt} = \dot{m}_c \quad \ldots (3.39)$$

Applying conservation of energy gives:

$$\frac{dU_a}{dt} = \dot{m}_c h_{fs} \quad \ldots (3.40)$$

Where

$$U_a = m_a u_{fae} \quad \ldots (3.41)$$

Carrying out the differentiation of both sides of Eq (3.40) gives:

$$\frac{dU_a}{dt} = m_a \frac{du_{fae}}{dt} + u_{fae} \frac{dm_a}{dt} \quad \ldots (3.42)$$

Substituting Eqs. (3.39), (3.40) into (3.42);

$$m_a \frac{du_{fae}}{dt} = \dot{m}_c \left(h_{fs} - u_{fae}\right) \quad \ldots (3.43)$$

Applying chain rule to the derivative and re-arranging gives:

$$\frac{dT_a}{dt} = \left[m_a \frac{du_{fae}}{dT_a} \right]^{-1} \dot{m}_c \left(h_{fs} - u_{fae}\right) \quad \ldots (3.44)$$

Equation (3.39) and (3.44) can be solved by the fourth order Runge-Kutta method to get the mass and temperature of the accumulator.

3.5. Fluid Properties.

To eliminate the errors caused by using incorrect properties. These properties include saturation pressure, liquid density, vapor density, liquid viscosity, vapor viscosity, liquid thermal conductivity, vapor thermal conductivity, vapor specific heat, liquid specific heat. They are expressed as function of saturation temperature in the form of 5^{th}-order polynomial equations (see Appendix (A) for detail):

$$Y = \sum_{n=0}^{n=5} A_n T_{SAT}^n \quad \text{... (3.45)}$$

Where (Y) represents a fluid property and (A_n) are the corresponding polynomial coefficients.

3.6. Efficiency of the system for heat transport.

From the working principle of the system, it can be seen that the useful energy is that delivered to the condenser, while the wasted energy is that through the vapor line, the shell of the condenser, the liquid line and the accumulator vessel. Insulating the vapor line and the condenser shell can minimize the energy loss. It is not recommended to insulate the liquid line or the accumulator vessel; for one needs a few degrees of temperature sub-cooling throughout the line and hence, avoiding heating the liquid inside the accumulator.

During the pumping time, the efficiency is larger than that of the charging time although the same power supply is maintained, since the vapor mass flow rate during the latter period is less than that of the former period .The reason that a large portion of (input power) goes in to heating the cold liquid which enters the boiler from the accumulator.

EFFICINCY=(Useful Energy Delivered to the Condenser/Total Energy Out put to The System)*100

Therefore,

$$EFFICIENCY(\%) = \frac{\sum_i \dot{Q}_{cc}(t)\Delta t}{\sum_i \dot{Q}_b(t)\Delta t} \times 100 \quad \text{... (3.46)}$$

Where,

$\dot{Q}_{CC}(t)$ is the sum of the vapor condensation energy rate plus the liquid sub-cooing energy to the cooling water.

Since the input power, Qb, in (W) is constant throughout the operation time then

$$EFFICIENCY(\%) = \frac{\sum_i \dot{Q}_{cc}(t)\Delta t}{\dot{Q}_b \sum_i \Delta t} \quad \text{...(3.47)}$$

Therefore,

$$\sum \Delta t = t_T \quad \text{...(3.48)}$$

$$(EFFICIENCY)_{TOTAL}(\%) = \frac{\sum_i \dot{Q}_{cc}(t)\Delta t}{(\dot{Q}_b)t_T} \quad \text{... (3.49)}$$

Equation (3.49) found [19].

3.7. The computer program.

A computer program was developed to evaluate the pressure and temperature for boiler, condenser and accumulator and also evaluate mass in the boiler, condenser and accumulator and exit water temperature, efficiency. The flow chart of the program is given in Fig.(3-3).

3.8 .Calculations procedure.

The general scheme of the program is to choose values for the independent variables:

- The vertical distance between condenser and accumulator (H).
- The vertical distance between boiler and condenser (L).
- Heat applied (Q_b=input power).
- Cooling water inlet temperature (T_{ic}).
- The ambient temperature (T_a).
- Mass flow rate of water.

The initial value of::

- Temperature of boiler, condenser and accumulator and masses of fluid are given.

The outputs of the program can be calculated are:

- Temperature profile of boiler, condenser and accumulator.
- Pressure of boiler, condenser and accumulator.
- Masses of fluid in the boiler and accumulator.
- Exit water temperature.
- Efficiency of the system.

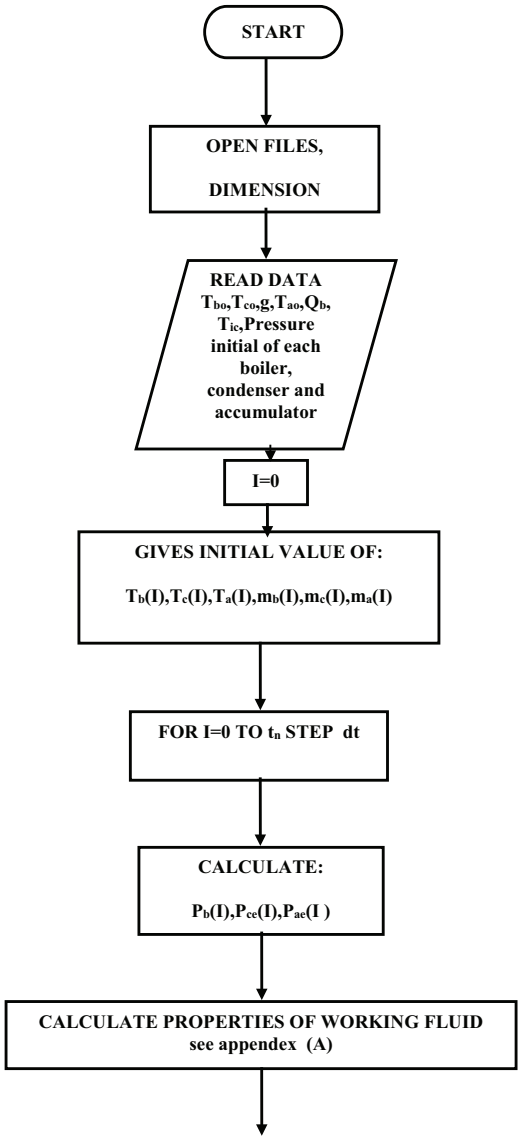

CONTINUED

Fig.(3-3) : Flow Chart of Computer Program.

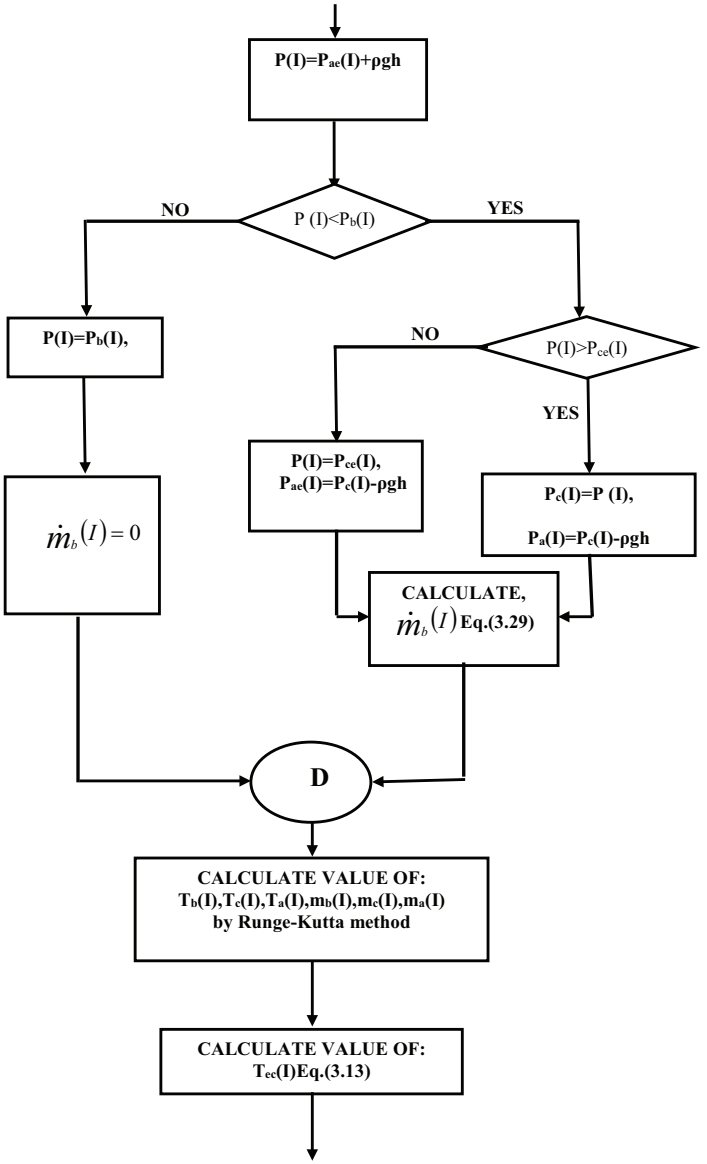
P(I)=Pae(I)+ρgh
NO
P (I)<Pb(I)
YES
P(I)=Pb(I),
NO
P(I)>Pce(I)
YES
P(I)=Pce(I),
Pae(I)=Pc(I)-ρgh
Pc(I)=P (I),
Pa(I)=Pc(I)-ρgh
$\dot{m}_b(I)=0$
CALCULATE,
$\dot{m}_b(I)$ Eq.(3.29)
D
CALCULATE VALUE OF:
Tb(I),Tc(I),Ta(I),mb(I),mc(I),ma(I)
by Runge-Kutta method
CALCULATE VALUE OF:
Tec(I)Eq.(3.13)

CONTINUED

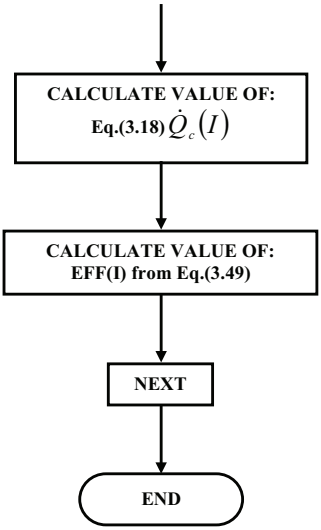
CALCULATE VALUE OF:
Eq.(3.18) $\dot{Q}_c(I)$
CALCULATE VALUE OF:
EFF(I) from Eq.(3.49)
NEXT
END

Results and Discussions

4.1. Results of the model.

Results of the transient model are obtained by using the following key dimensional and operational parameters, which are fixed for all cases shown in table (4-1).

i. The mass in the boiler, (m_b=4 kg).

ii. The initial temperatures in boiler, condenser and accumulator are (T_b=T_c=T_a=20°C).

iii. The initial pressures in boiler, condenser and accumulator are (P_b=P_c=P_a=1bar).

iv. The inlet cooling water temperature is (T_{ic}=20°C).

v. The surrounding temperature is (T_s=20 °C).

CASES	*WORKING FLUID*	*HIEGHT(m)*	*INPUT POWER(W)*	*MASS FLOW RATE OF COOLING WATER(kg/s)*
EFFECT OF HIEGHT	*R-11*	*15,10,6*	*2000*	*0.015*
EFFECT OF INPUT POWER	*R-11*	*15*	*2500, 2000, 1500, 1000*	*0.015*
EFFECT OF CHANGE MASS FLOW RATE OF WATER	*R-11*	*15*	*2000*	*0.07, 0.03, 0.015*
EFFECT OF WORKING FLUID	*R-114*	*15*	*2000*	*0.015*

Table (4-1) parameters investigated in the work.

4.2. Base case results.

Figures (4-1, 2) shows the cyclic operation of the loop heat pipe. The operation cycle consist of three stages. The initial stage which is known as the no pumping zone (NPZ), during which no flow takes place between the boiler and condenser and only heating process of working fluid is takes place. During the second stage which is known as the transitional zone (TZ) vapor flows between the boiler and condenser. The vapor is condensed initially inside the condenser at constant condenser pressure and no flow occurs between the condenser and the accumulator. The third stage known as the pumping zone (PZ) or some this known as the effective pumping zone. During this stage flow of condensed working fluid occurs between the condenser and the accumulator. This stage ends when all the predetermined circulated mass is completely transferred to the accumulator. When the cycle is complete the instantaneous charge process starts where the float valve between the accumulator and boiler is opened the predetermined mass of working fluid to the transferred for the accumulator to the boiler. At the end of this process a new cycle is started.

The variations of performance parameters of the loop heat pipe is shown in Fig. (4-3). the working fluid is (R-11), the height between condenser and accumulator is (15 m), the input heat to the boiler is (2000W) and the cooling water flow rate is (0.015 kg/s).

The figure shows that no pumping zone (NPZ) duration is about (324.51sec), Fig. (4-3), there is no flow between the boiler and the condenser. During this period the working fluid in the boiler is heated from the initial temperature to the saturation temperature at the prevailing pressure in the boiler. It is noticed that the pressure inside the boiler increases from (1bar) to the pumping pressure is (3.08 bar), Fig. (4-4). The pumping process start when the boiler temperature reaches (59.41ºC), Fig. (4-3) which is the saturation temperature at boiler pressure (3.08 bar). Fig. (4-5) show the variations of mass between boiler and accumulator. The mass in the boiler decreases but the mass in the accumulator

increases. Fig. (4-6) shows that the cooling water temperature of (20ºC) to a maximum value (49.76ºC) at the end of cycle duration heat exchanging between working fluid and cooling water. It can be seen from this figure that the cycle duration is about (1100sec). Fig. (4-7) shows the mass flow rate of working fluid between the boiler and the condenser increases from zero and reaches a maximum value of ($1.44*10^{-2}$ kg/s) at time of (1100sec).

4.3. Parametric study.

4.3.1. Effect of height.

The condenser is water-cooled and is made of coiled copper tubing of (6.35 mm) diameter comprising (0.4 m^2) of surface area. The condenser shell, the boiler and the accumulator are all made of (76.2 mm) diameter copper pipe. The diameter of the pipe connecting the accumulator to the boiler via the check valve is (9.52 mm).

The mass inside the boiler starts to heat up in order to build up the saturation pressure towards the target pressure. The minimum lifting pressure, equals to ($P = P_{ae}+\rho_s gH$) =3.08 bar, and the lifting temperature, T_b=59.41°C (saturation temperature of lifting pressure), where (P_{ae} is saturation equilibrium pressure of accumulator). This is no pumping zone in which literally all the input power goes into heating the working fluid.

The condenser pressure is equal the boiler pressure during the no pumping zone (NPZ). The condenser temperature, however, is not affected by the heating in the boiler yet. Line (A1-B1) in Fig. (4-3) illustrated the duration of no-pumping zone which is from starting operation of the system until the starting of the transitional zone (i.e. time of no-pumping zone = 324.51 sec = 5.4 min.). In the no-pumping zone ($P_b \leq P$). The accumulator temperature and pressure are still at their initial saturation values, since no input to the accumulator has arrived yet, and there is no flow out of it.

Once T_b exceeds $T_b(P)$ where ($T_b(P)$ saturation temperature at saturation pressure) vapor starts to flow out of the boiler to the condenser. This marks the

beginning of the transitional zone (TPZ). Figure (4-3) shows the transitional zone temperature inside the condenser, (line B1-C1) where it increases to approach the saturation temperature at saturation pressure (P) at the end of the transitional zone.

Figure (4-4) shows the transitional zone pressure inside the condenser, (line BB1-CC1), where its value remains constant at (P). In the transitional zone ($P_{ce} \leq P < Pb$) where (P_{ce} is saturated equilibrium pressure in the condenser) the time of the transitional zone is equal (450.98 sec =7.5 min.). Therefore, it may be concluded that the condenser pressure controls the boiler pressure and temperature. It also controls the accumulator pressure, maintaining it at almost saturation pressure (P_{ae}) where (P_{ae}) is saturation equilibrium pressure in the accumulator at saturation temperature in the accumulator.

Since the working liquid is flowing now into the accumulator, the accumulator temperature increases very slightly since the entering liquid is sub-cooled to a near ambient temperature.

Once the condenser temperature exceeds the saturation temperature, then the pressure inside the condenser increases along the saturation vapor-pressure curve. This is a characteristic of the pumping zone (PZ) see Fig. (4-3) and Fig. (4-4) line (C1-D1) and (CC1-DD1). The temperature of the boiler at the end of the pumping zone is (T_b= 90.78°C) and the condenser is (T_c= 81.17°C) and also the pressure in boiler is (P_b= 6.73 bar) and the condenser pressure (P_c= 5.38 bar). As was the case with the transitional zone, the condenser pressure controls the accumulator and boiler pressure. Since the condenser saturation pressure (P_{ce}) increases with saturation temperature, then the accumulator pressure starts to increase appreciably in the pumping zone; as the pressure at the accumulator inlet is equal to ($P_{ae}= P_{ce}-\rho_s gH$).

The end of the pumping zone is triggered by the opening of the float valve nozzle when the working fluid level in the boiler drops to a predetermined value.

At this point, recharging of the boiler from the accumulator takes place through a liquid line connecting them via a check valve.

Flashing takes place inside the boiler due to a depressurization of the relatively high-pressure boiler through the equalization vapor line connecting it to the lower pressure accumulator.

Flashing process can be made very briefly by a proper sizing of the vapor line connecting the accumulator to the boiler, i.e., increasing its diameter to increase the vapor mass flow rate to the accumulator, and by increasing the diameter of the liquid line connecting the accumulator to the boiler.

This leads to a more flow of the relatively cold working liquid goes into the boiler to hinder the flashing process and lowering the amount of superheating of the working fluid in the boiler.

Therefore, the flashing process becomes a very short transient in comparison with the much slower charging time. The flashing process effect may then be safely neglected.

The variation of mass in the boiler and accumulator is shown in Fig. (4-5). The mass inside the boiler decreased due to the evaporation of working fluid after evaporating the vapor flowing to the condenser in the condenser the vapor condensation and flow to the accumulator therefore the mass in accumulator increased. The mass in the condenser is constant. This figure shows three different stages.

The outlet temperature of the cooling water in the condenser, the temperature is [T_{ec} =49.76°C] as shown in Fig. (4-6).

The variation of mass flow rate leaves the boiler to the condenser is shown in Fig. (4-7).

It can be observed by comparing the present work in Fig. (4-3,4,5) with the experimental data and theoretical model of **Gari *et al***,[19], in Fig.(4.42), (4.43) and (4.44) respectively, that the present work predictions have the same behavior of the transient curves of the experimental work of the above motioned reference.

In these cases all operating parameters are kept the same of previous cases while the accumulator height changed (i.e., H). Fig. (4-8) shows the operation temperatures of boiler and condenser of height of (10 m). The temperatures of the boiler and the condenser decreased when the accumulator height decreased. Also the no-pumping duration decreases and the efficiency of the system. The comparison of Figs. (4-3,4) with (4-8) and (4-9) show that the temperature decrease as the height is reduced. The Figures also show that the duration of no-pumping zone decreases as the height is decreased, since the pressure at which vapor flow rate boiler to condenser decreases.

The results when using height of accumulator (10 m) is [T_b=85.74°C, T_c=79.08°C and t_{np}=234.2 sec]. The results when using (H=6m) as show in Fig. (4-10) and (4-11), [T_b=81.54°C, T_c=77.55°C and t_{np}=152.7 sec]. The time required to complete one cycle when (H=15m) is [1100 sec], in (H=10m) is [1050 sec] and in (H=6m) is [1010 sec]. Figures, (4-12), (4-13), (4-14) and (4-15), mentioned variations the temperature of boiler, temperature of condenser, pressure of boiler and pressure of condenser. The temperature of boiler increased when the height is increased. The temperature of condenser increased when the height is increased but the no-pumping zone decreased. The pressure of the boiler increased when the height is increased but the no-pumping zone decreased when the height is decreased also pressure of condenser.

4.3.2. Effect of input power.

This case utilizes the same long heat pipe passive condensate pumping system set-up in case (4.3.1), but with a different energy input to the boiler and the same working fluid and mass flow rate of cooling water. The maximum temperature of boiler and condenser decreases when the input heat decreases. At a heat input of (1000 W) temperature of boiler and condenser become (72.96°C and 66.4°C) respectively.

Also the duration of the no-pumping zone increases as the input heat decreases, see Fig. (4-16) and (4-17), since the working fluid requires longer time

to reach the evaporation temperature at a low heating rate. The other hand, the maximum temperature of boiler and condenser increase with increasing heat input and the duration of the no-pumping zone becomes shorter as shown in Figs. (4-18) and (4-19) when using input heat (1500W) and Figs. (4-20) and (4-21) when using input heat (2500W). The results of the present case compared with the previous case when using the same height and mass flow rate of water but with different input heats. Figures, (4-22), (4-23), (4-24) and (4-25), mentioned variations the temperature of boiler, temperature of condenser, pressure of boiler and pressure of condenser. The temperature of boiler increased when the input heat is increased. The temperature of condenser increased when the input is increased but the no-pumping zone decreased. The pressure of the boiler increased when the input heat is increased also pressure of condenser but the no-pumping zone increased when the input is decreased.

4.3.3. Effect of mass flow rate of cooling water.

In these cases the mass flow rate of cooling water is changed while all other variables are kept constant. Two mass flow rates are used namely (0.03 kg/s and 0.07 kg/s). It is seen that the maximum temperature of the condenser decreases as the mass flow rate increases as shown in Figs. (4-26, 27) and (4-28, 29) respectively while the maximum temperature of boiler remains approximately, constant. The thermal efficiency of the system is also increases.

4.3.4. Effect of working fluid.

In this case different working fluid is used namely (R-114) while all other variables remain unchanged. Since the latent heat of evaporation for (R-114) is much lower than that for (R-11) (roughly $\lambda_{R\text{-}114} = 0.6218*\lambda_{R\text{-}11}$), therefore, it is expected that the pumping time for (R-114) system is shorter than that of (R-11) system. The variation of temperature and pressure are illustrated in Figs. (4-30) and (4-31) respectively.

The behavior is the same as that of (R-11) but the time in the (NPZ) is shorter than of the time of (R-11). The no-pumping time in the present case is (197.0 sec).

Fluids of relatively lower vapor pressures (e.g. R-11) will attain the minimum pressure needed to lift the condensate to the accumulator ($P=P_{ae}+\rho_s gH$) at higher temperatures; i.e. the former fluids make the long heat pipe condensate system operates at relatively high temperatures while the latter fluids make the system operates at relatively low temperatures and high pressures (present case) as observed in Figures (4-30), (4-31) and (4-32).

Since (R-114) has a relatively high vapor pressure at low temperature, then it will attain the lifting pressure at lower T_b (and T_c). The efficiency of the system decreased when using the working fluid in the present case. The efficiency of the present work is (64.4%) but the efficiency of the previous case is (89.3%). The change of working fluids and effected on the operating system is show in Figs.(4-33,4-34,4-35,and 4-36).

4.4. Effect some parameter on the system operating.

1. The effect of the latent heat of evaporation on the operation of the system was examined by comparing case (4.3.1) and case (4.3.4) as shown in Fig. (4-3,4) and (4-30,31). Long heat pipe condensate pumping systems utilizing working fluids with relatively low latent heats of evaporation are characterized by shorter no-pumping period for a given circulating mass and input power. The reason is that since most of (Q_b) is carried by the vapor flow rate ***(input heat to the boiler≈latent heat of evaporation*mass flow rate of vapor)***, therefore, for a given Q_b: ***the vapor mass flow rate is inversely proportional to the latent heat of evaporation***. $\dot{m}_b \propto \frac{1}{h_{fg}}$

Hence, working fluids having lower latent heat will generate more vapor mass flow rates in order to compensate and be able to carry the input power. The pumping period which is inversely proportional to the vapor mass flow rate will, therefore, be shorter for fluids with lower latent heat of evaporation.

2. Figure (4-37) shows the variations of ($\Delta T=T_b-T_c$) with height at different input heats. It is seen the ΔT increases as the height is increased. The curve of ($\Delta T=T_b-T_c$) versus (H), is plotted for different input powers, Q_b (W). For relatively low heights, the boiler starts pumping vapor to the condenser at relatively low pressure (and hence low temperatures).

3. The effect of varying input power to the boiler, on the behavior of boiler and condenser temperatures is shown in Fig. (4-38). It can be seen that both (T_b) and (T_c) increased as (input heat) increased.

4.5. Efficiency of the system for heat transport.

From the working principle of the system, constructed by ***Gari et al*** .[19], it can be seen that the useful energy is that delivered to the condenser, while the wasted energy is that lost through the vapor line, the shell of the condenser, the liquid line and the accumulator vessel. Insulating the vapor line and the condenser shell can minimize the energy loss. It is not recommended to insulate the liquid line or the accumulator vessel; for one needs a few degrees of temperature sub-cooling throughout the line and hence, avoiding heating the liquid inside the accumulator. During the pumping time, the efficiency is larger than that of the charging time although the same power supply is maintained, since the vapor mass flow rate during the latter period is less than that of the former period. The reason that a large portion of (input power) goes in to heating the cold liquid which enters the boiler from the accumulator.

See Figs.(4-39),(4-40) and (4-41), it can be conclued that the efficiency increased when the mass flow rate of water increased and also the efficiency increased when the accumulator height increased. The circulation mass between the boiler and the accumulator increases the efficiency of the system increases too.

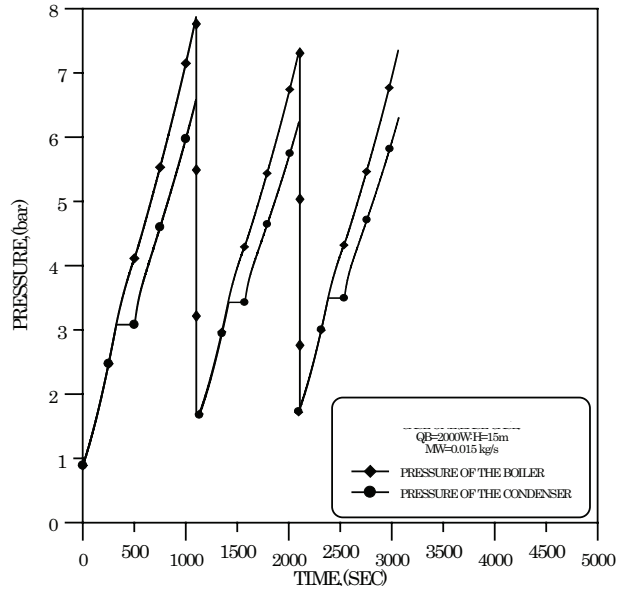

Fig. (4-1):Boiler and condenser pressure when the mass circulating between boiler and accumulator is 3kg.

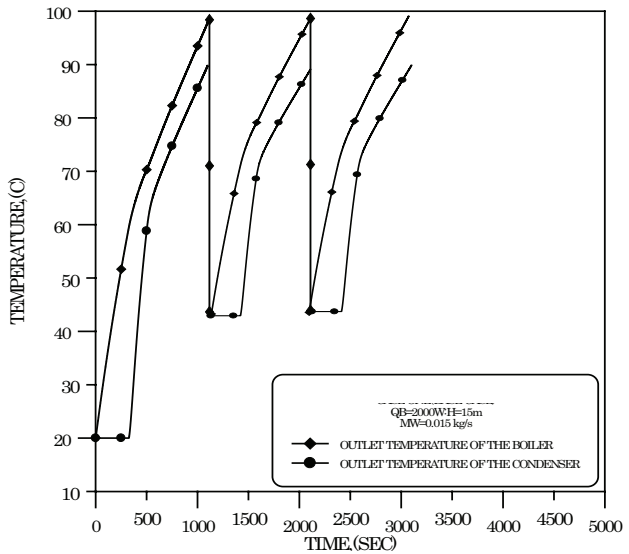

Fig. (4-2):Boiler and condenser temperature when the mass circulating between boiler and accumulator is 3kg.

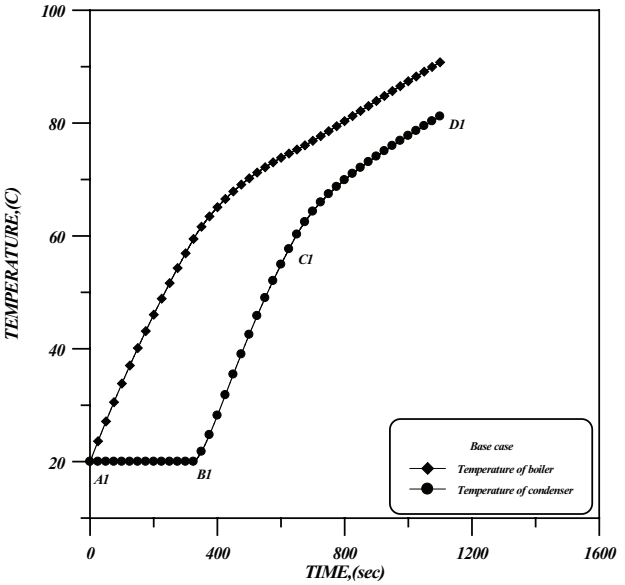

Fig. (4-3):Boiler and condenser temperature.

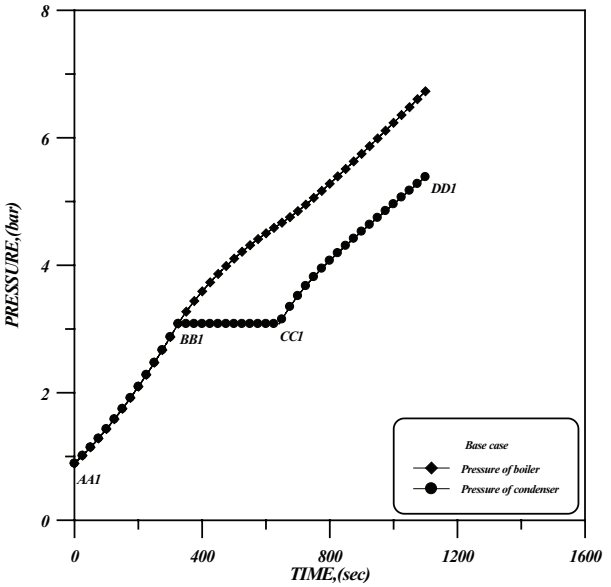

Fig. (4-4):Boiler and condenser pressure.

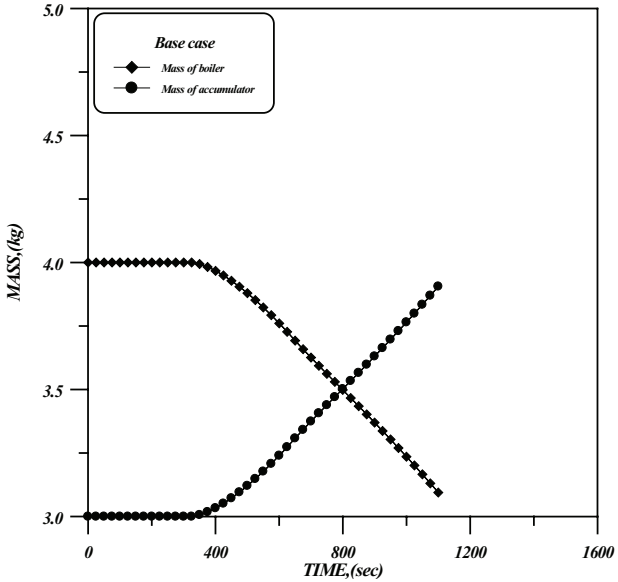

Fig. (4-5):Mass variations.

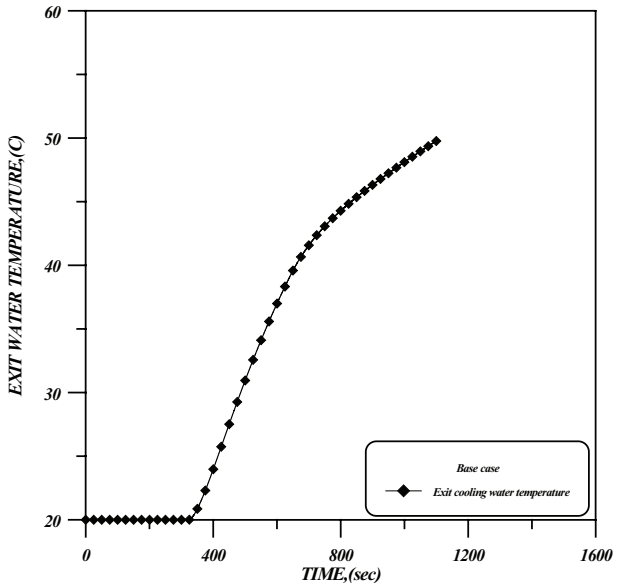

Fig. (4-6):Exit water temperature.

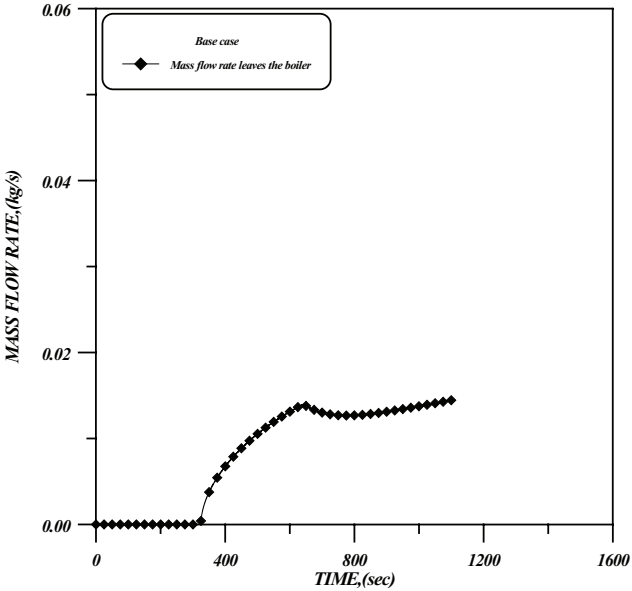

Fig. (4-7):Mass flow rate leaves the boiler.

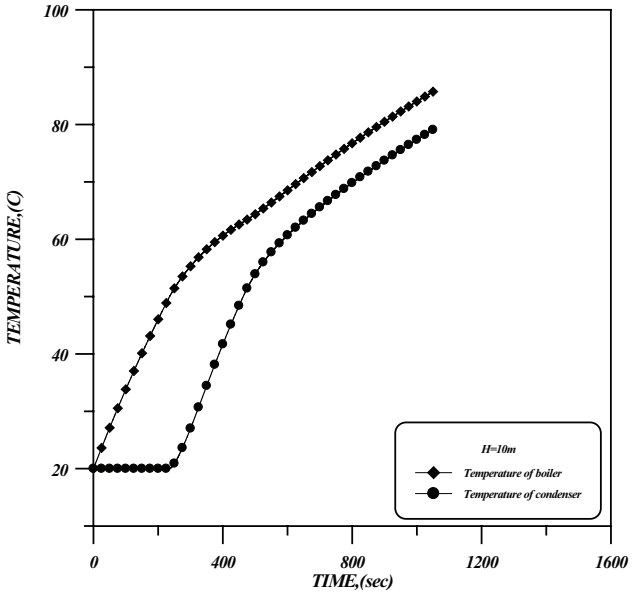

Fig. (4-8):Boiler and condenser temperature.

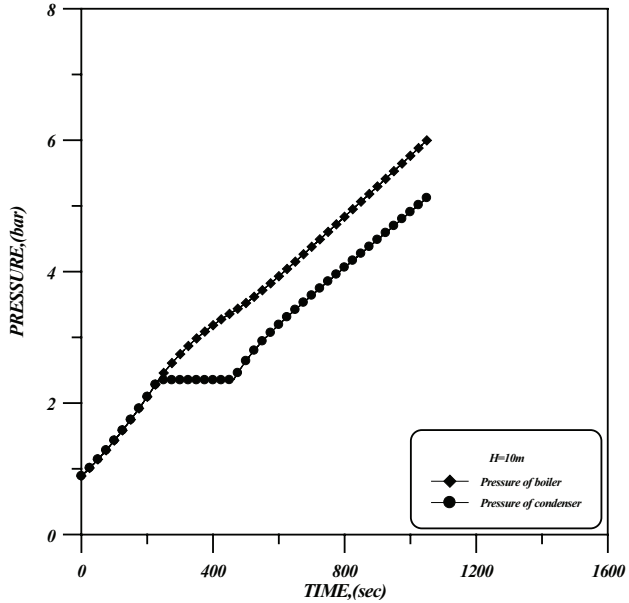

Fig. (4-9):Boiler and condenser pressure.

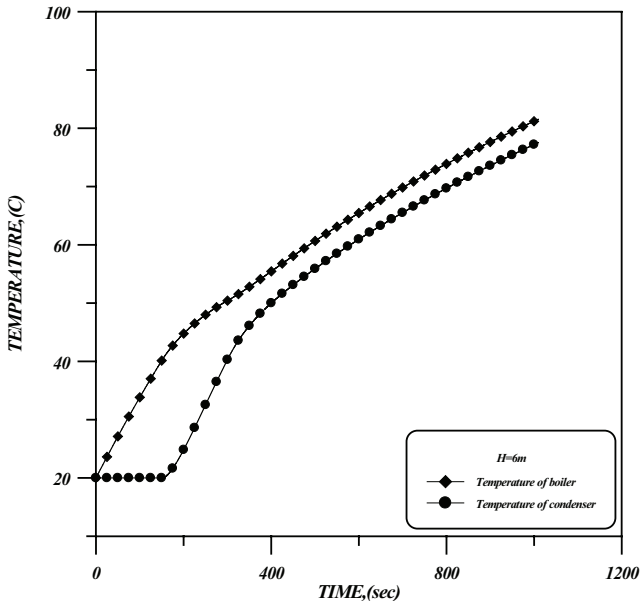

Fig. (4-10): Boiler and condenser temperature.

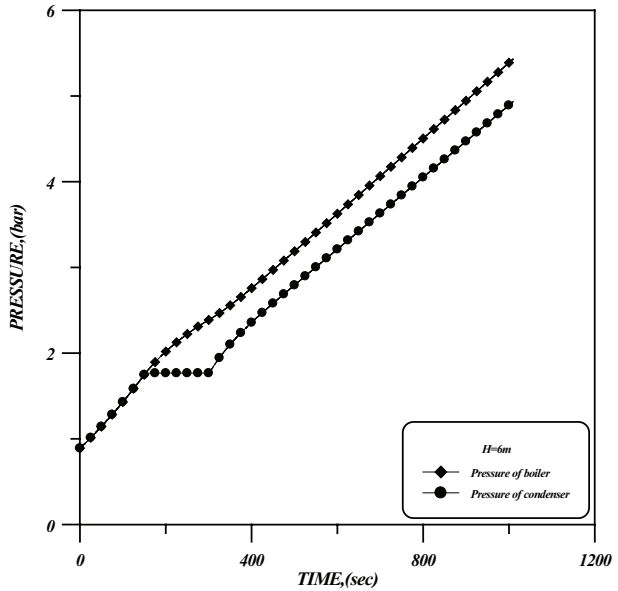

Fig. (4-11):Boiler and condenser pressure.

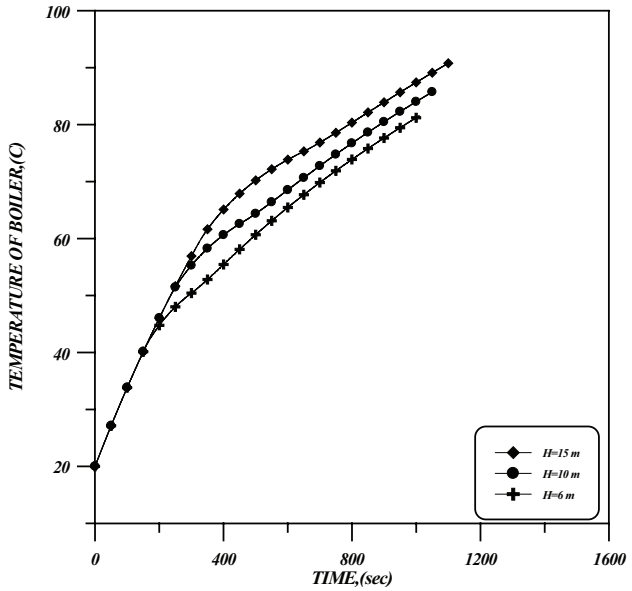

Fig. (4-12): Variations boiler temperatures when using different heights.

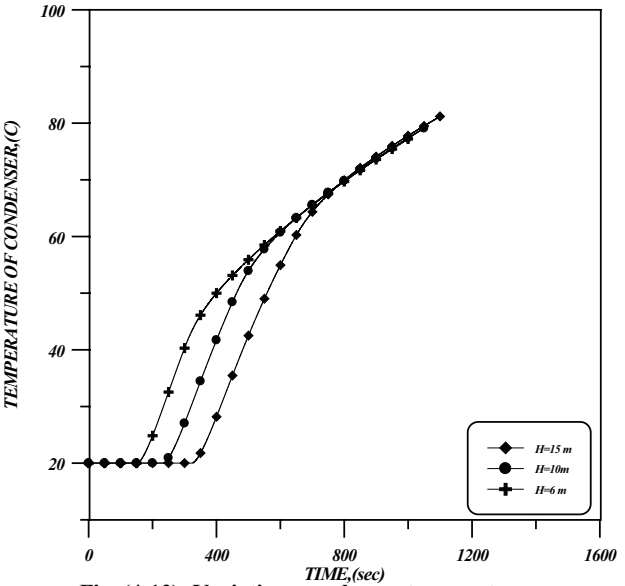

Fig. (4-13): Variations condenser temperatures when using different heights.

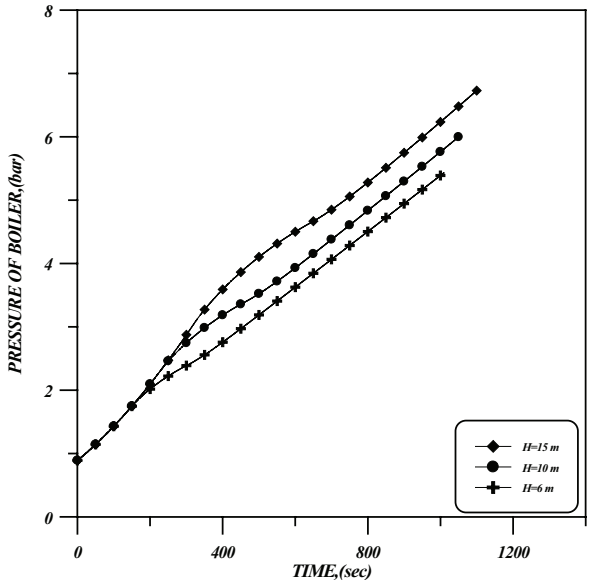

Fig. (4-14): Variations boiler pressures when using different heights.

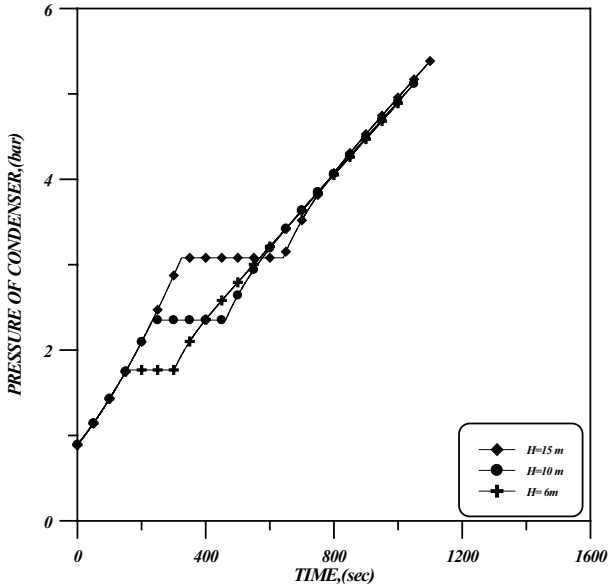

Fig. (4-15): Variations condenser pressures when using different heights.

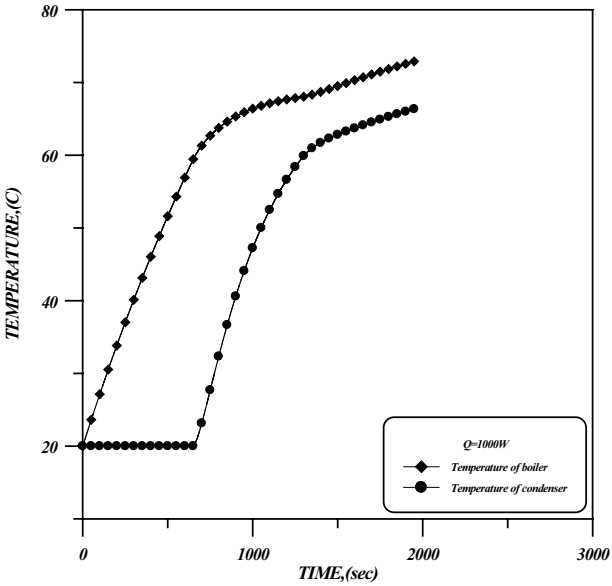

Fig. (4-16):Boiler and condenser temperature.

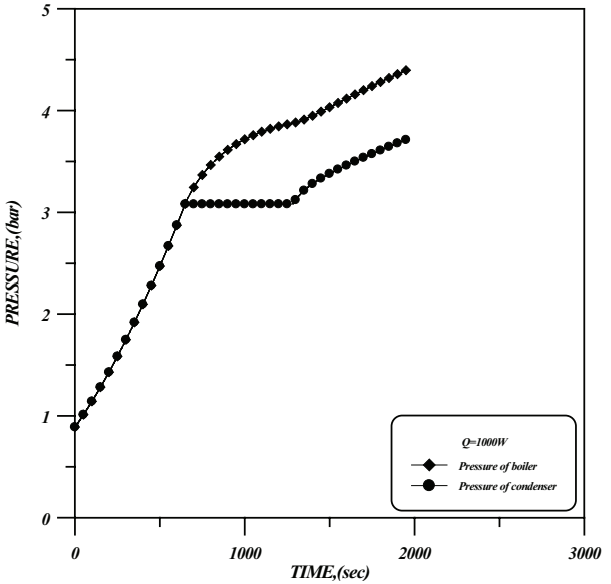

Fig. (4-17): Boiler and condenser pressure.

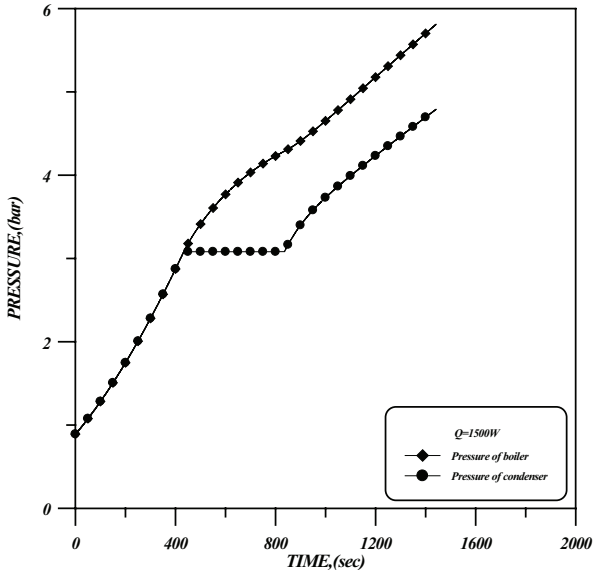

Fig. (4-18): Boiler and condenser pressure.

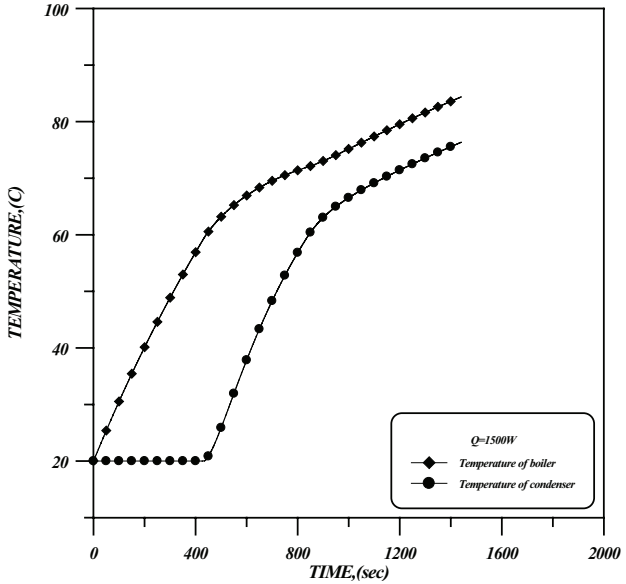

Fig. (4-19): Boiler and condenser temperature.

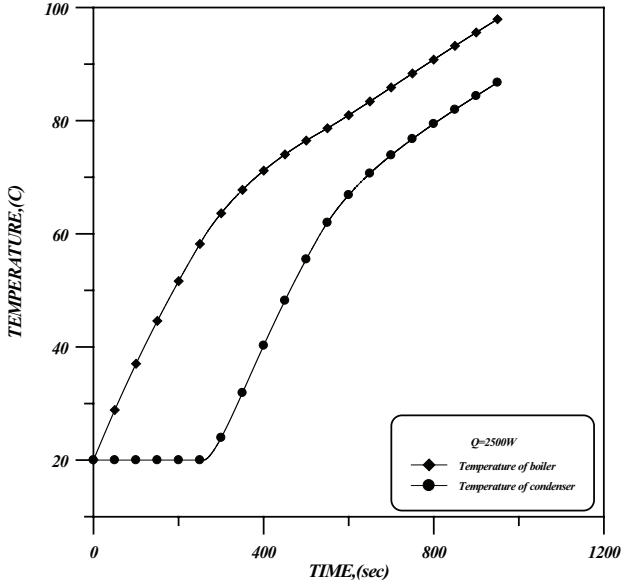

Fig. (4-20): Boiler and condenser temperature.

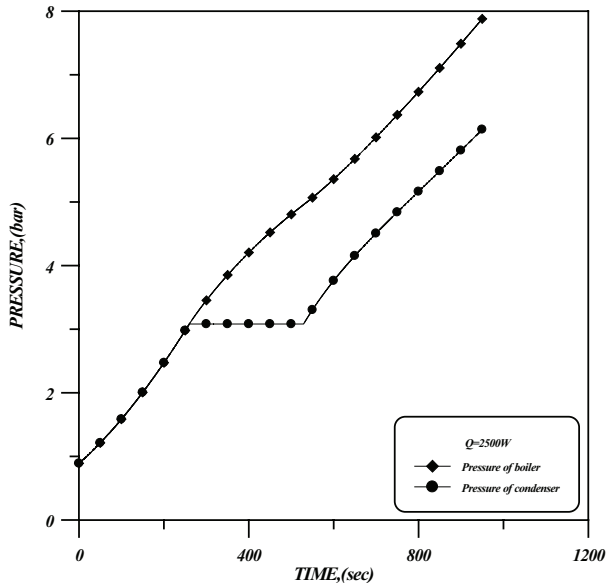

Fig. (4-21): Boiler and condenser pressure.

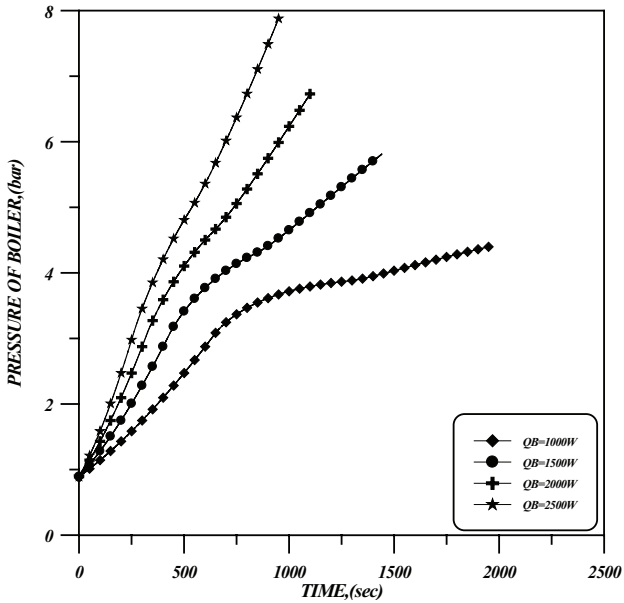

Fig. (4-22): Variations boiler pressures when using different input heats.

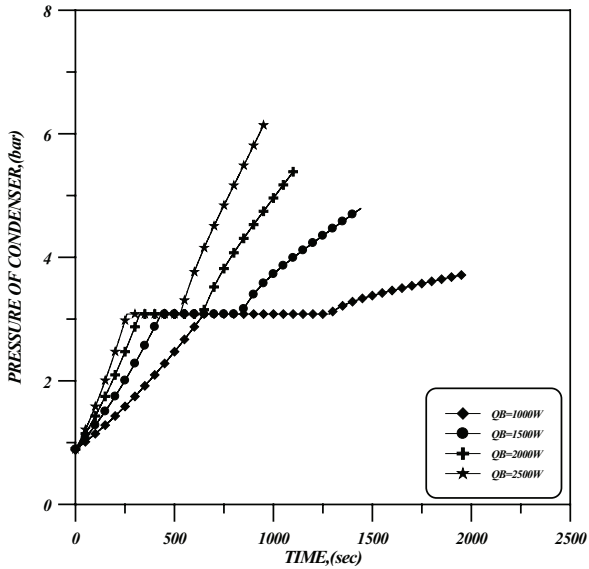

Fig. (4-23): Variations condenser pressures when using different input heats.

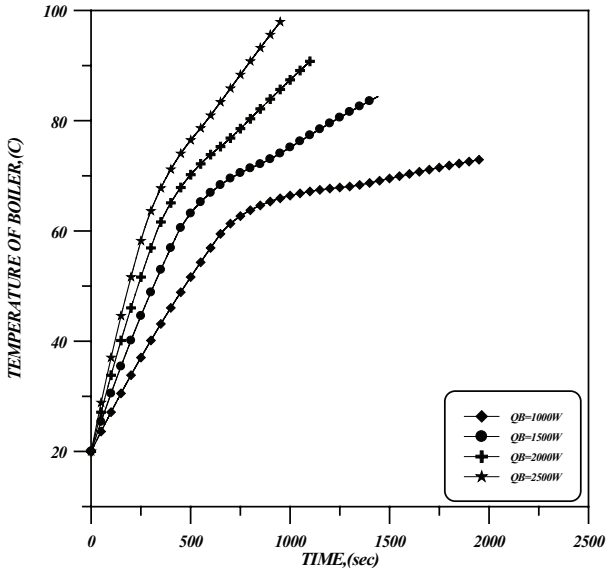

Fig. (4-24): Variations boiler temperatures when using different input heats.

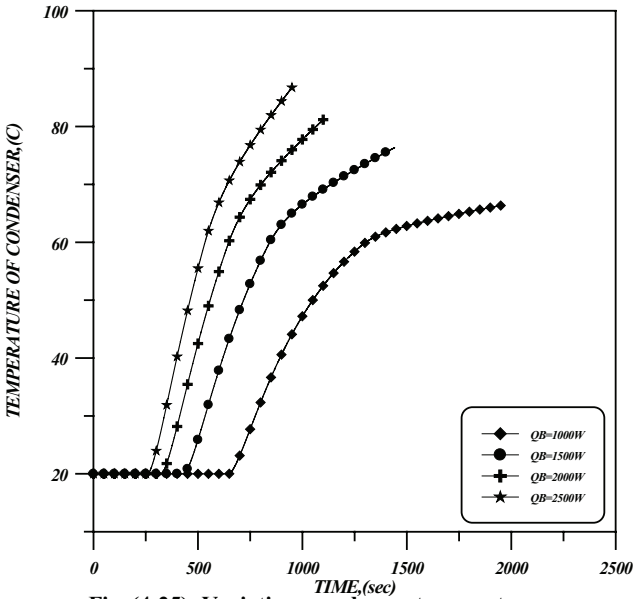

Fig. (4-25): Variations condenser temperatures when using different input heats.

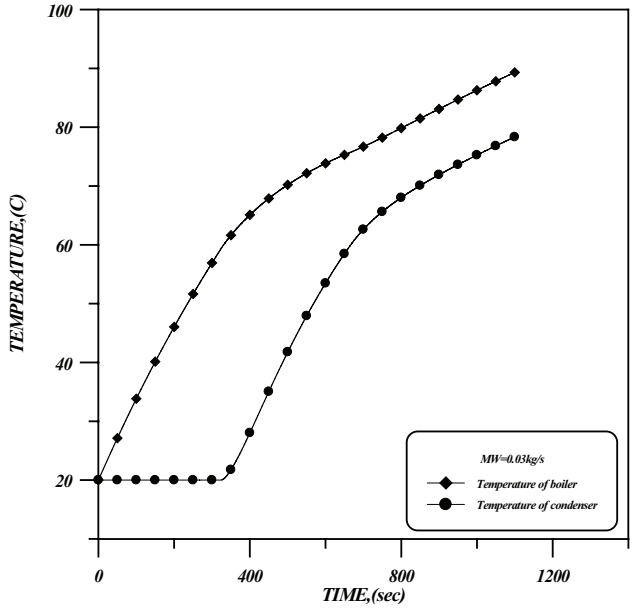

Fig. (4-26):Boiler and condenser temperature.

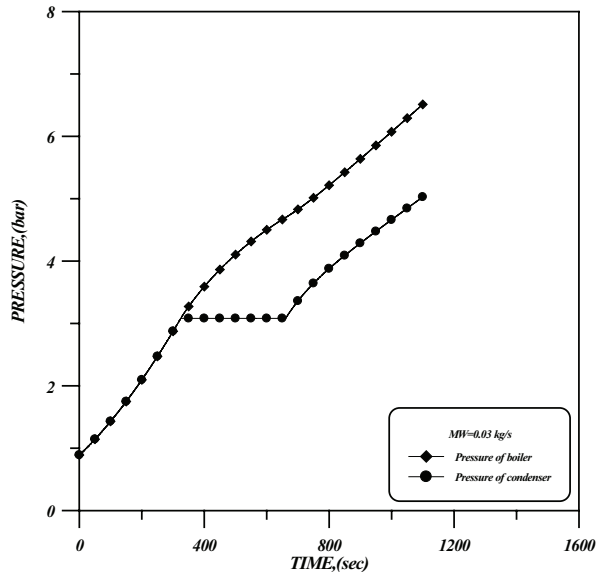

Fig. (4-27):Boiler and condenser pressure.

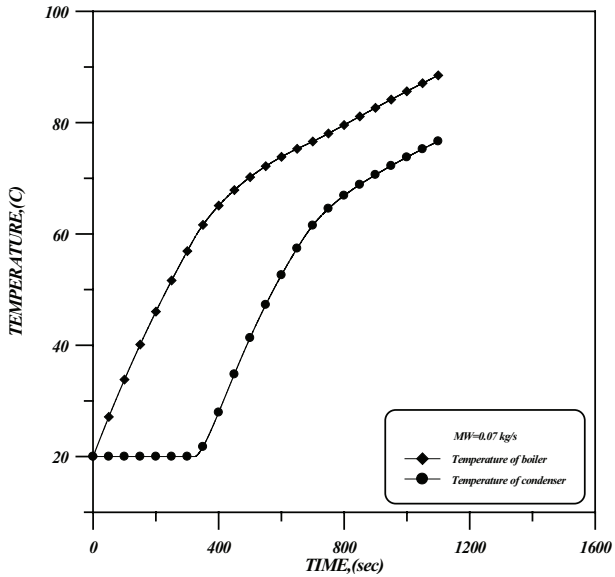

Fig. (4-28):Boiler and condenser temperature.

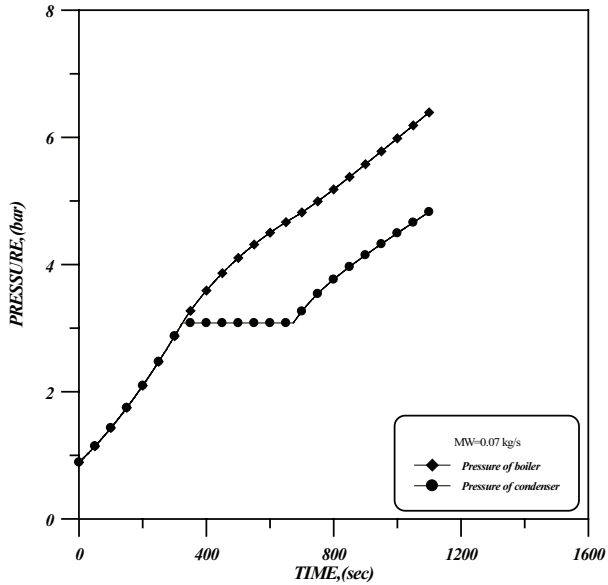

Fig. (4-29):Boiler and condenser pressure.

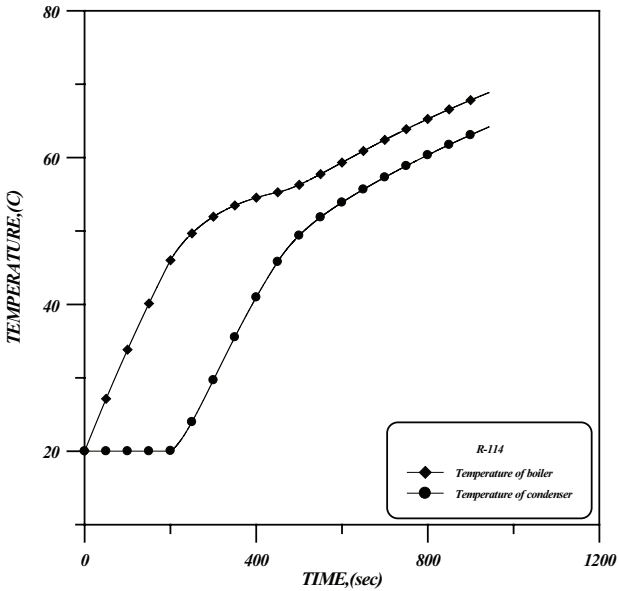

Fig. (4-30): Boiler and condenser temperature.

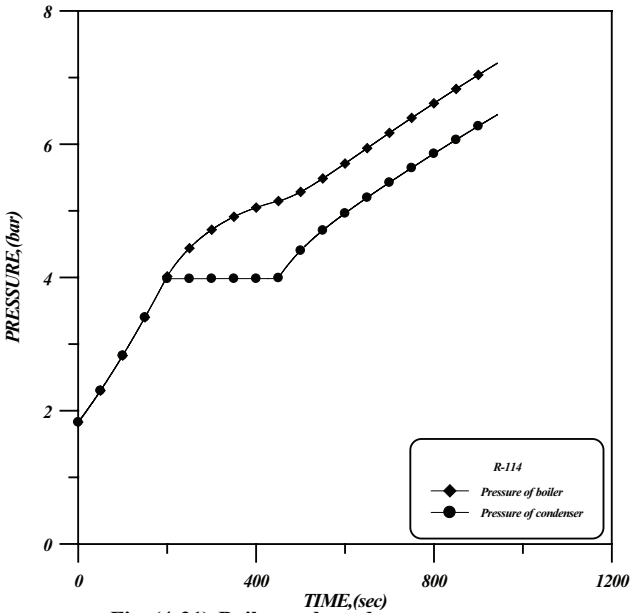

Fig. (4-31):Boiler and condenser pressure.

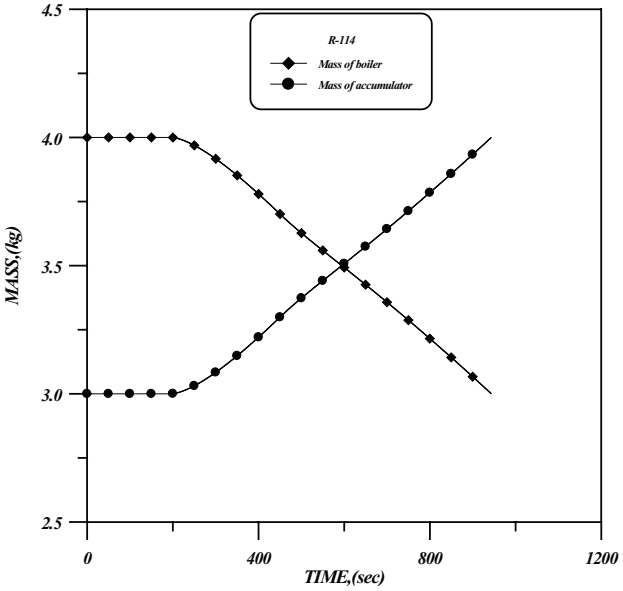

Fig. (4-32):Mass variations.

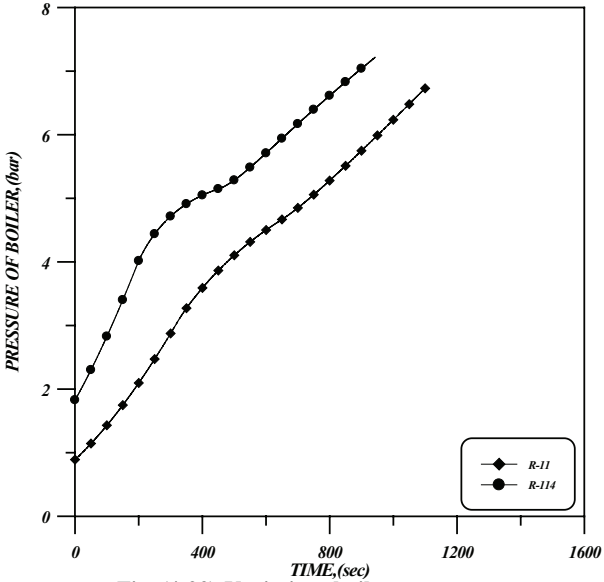

Fig. (4-33):Variations boiler pressure when using different working fluids.

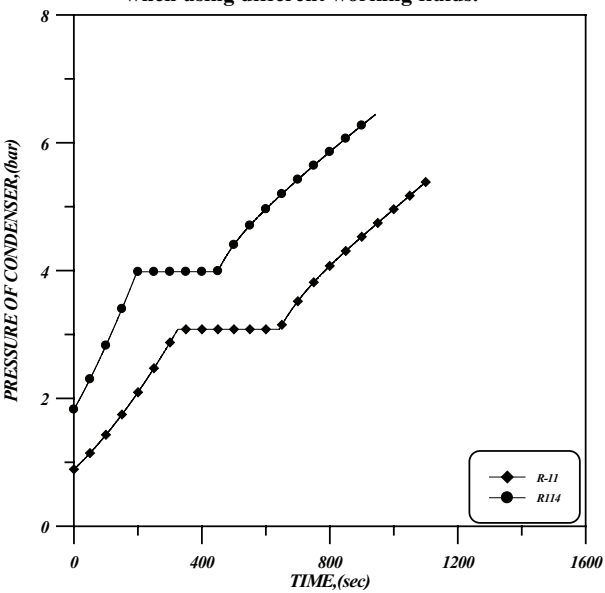

Fig. (4-34):Variations condenser pressure when using different working fluids.

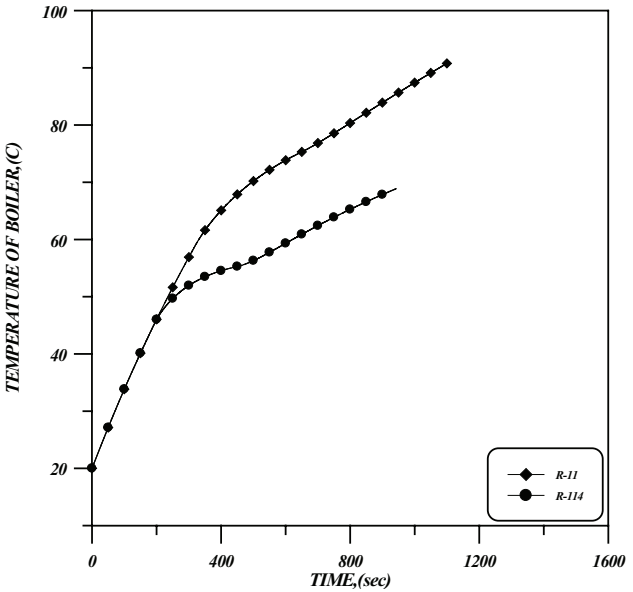

Fig. (4-35):Variations boiler temperature when using different working fluids.

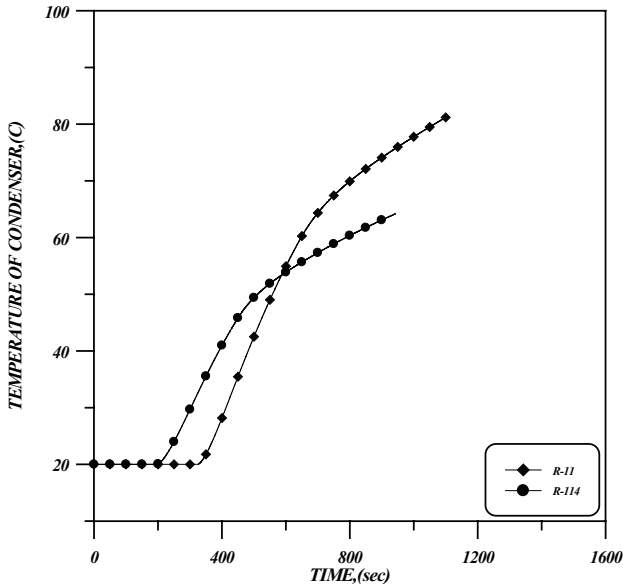

Fig. (4-36): Variations condenser temperature when using different working fluids.

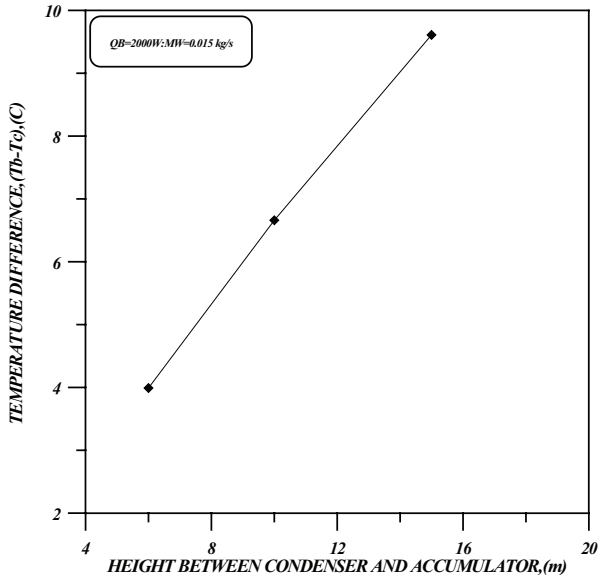

Fig. (4-37):Variations temperature difference with height.

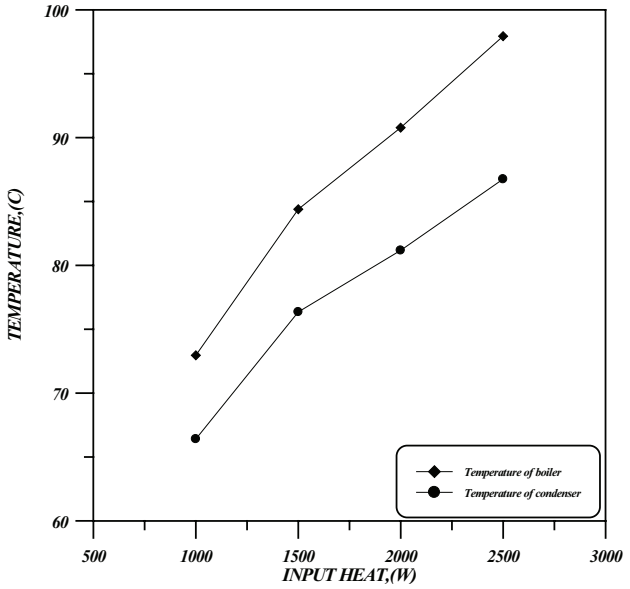

Fig. (4-38):Variations temperatures of boiler and condenser with input heat.

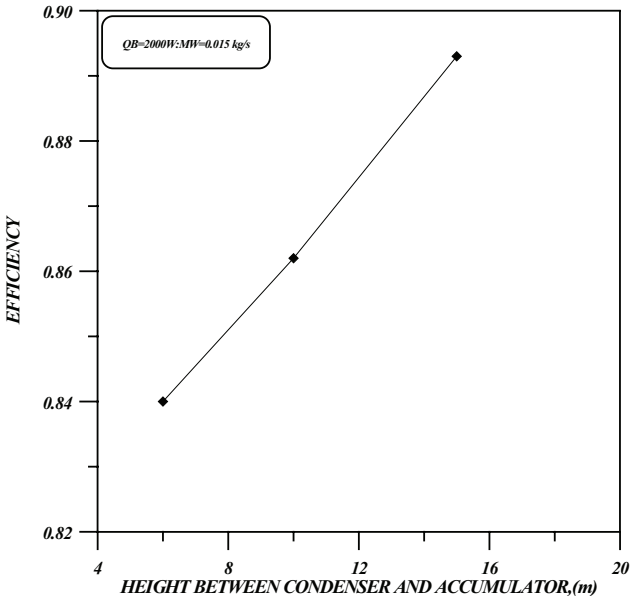

Fig. (4-39):Variations efficiency with height.

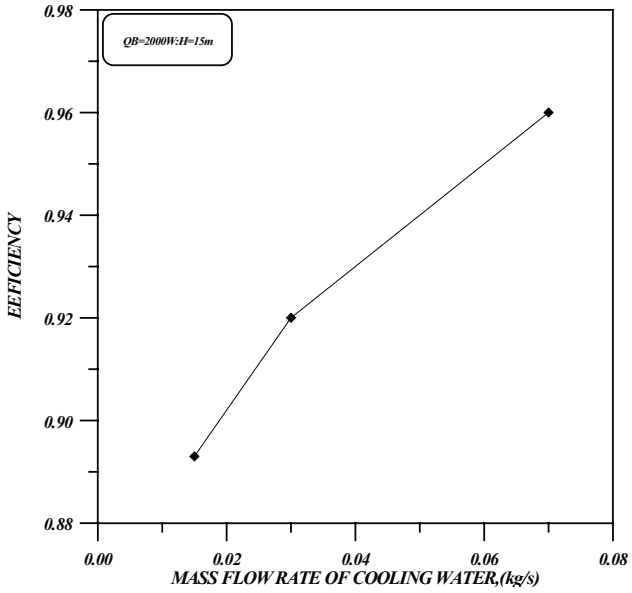

Fig. (4-40): Variation efficiency with mass flow rate of water.

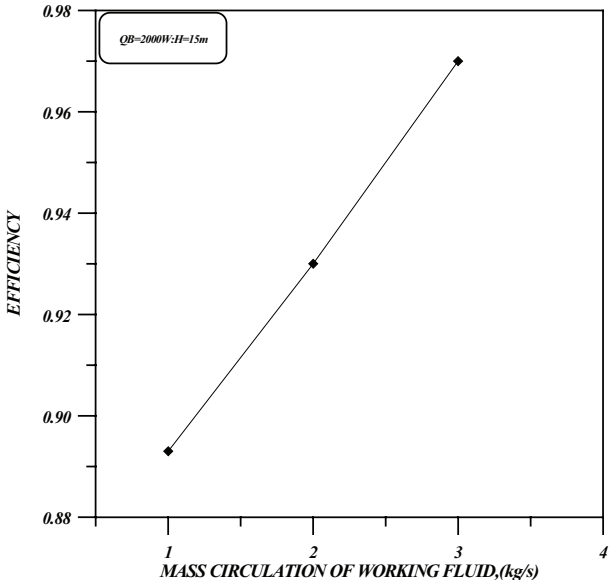

Fig. (4-41):Variations efficiency with mass circulation of working fluid.

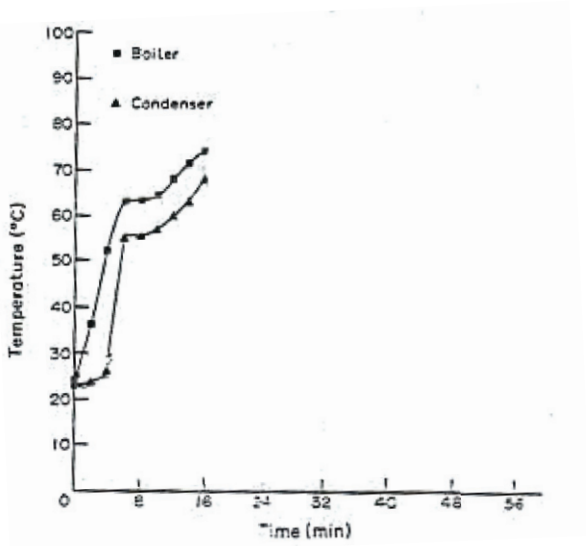

Fig. (4-42): Experimental data of acetone system obtained by **Gari *et al***, [19]

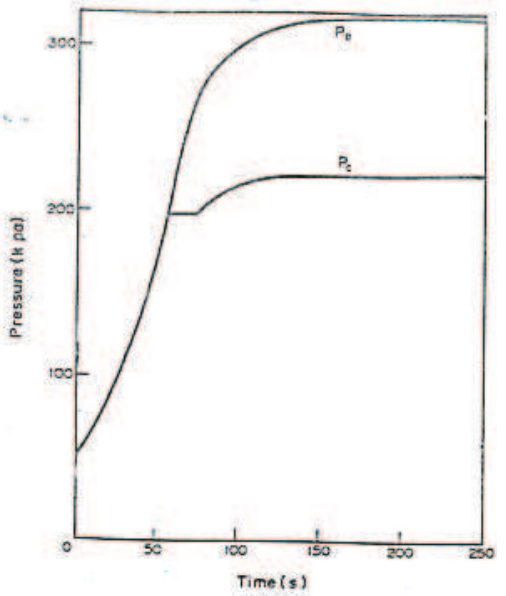

Fig. (4-43):Simulation for pressures of boiler and condenser of acetone system of acetone system obtained by **Gari *et al***, [19]

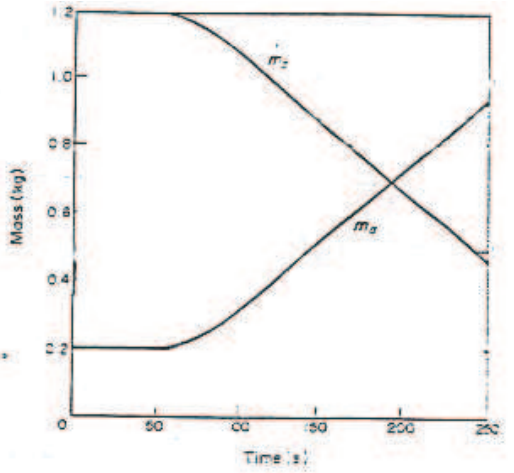

Fig. (4-44): Simulation for masses of boiler and condenser of acetone system of acetone system obtained by **Gari *et al***, [19]

Conclusions and Recommendations

5.1 Conclusion.

Throughout the present work, the following main conclusions have been drawn:

1. The efficiency for case (R-11, 2000W, H=15m) is 89.3%, of the long heat pipe passive condensate pumping system with the superior heat carrier (vapor) but the efficiency of (R-114, 2000W, H=15m) is 64.4%, therefore, the selection of working fluid effects the efficiency of the system.
2. Fluids with higher latent heat of evaporation for (e.g. R-11) are recommended for relatively long pumping periods (18.33 min.).
3. The working fluids having a lower liquid density are preferred in great heights, in order to reduce the static pressure head ($\rho_s gH$), along the liquid line.
4. Working fluids of high vapor pressures at relatively moderate temperatures (e.g. R-114) are recommended to be utilized in long heat pipe passive condensate pumping of great heights (above 10m) so that the system operates at relatively moderate operational temperatures (T_b and T_c). On the other hand for low heights (below 10m), it is recommended to utilize working fluids of relatively moderate pressures at relatively high temperatures (e.g. R-11), so that, the system operates at the desired operational temperatures as those for great heights.
5. The mass flow rates of cooling water increased the efficiency of the system increased. Also increased the efficiency when the height of accumulator increased.

5.2 Recommendations for Further Work.

1. Design and built a passive condensate pumping system and measured the temperatures of boiler and condenser experimentally.

2. Design and build a LHP with sufficient devices to measure pressure drops along the system and mass flow rate.

3. The application of the more sophisticated void propagation model to the condenser is recommended for further investigation method of analysis.

References

[1]- P.D. Dunn and D.A. Reay, "***Heat Pipes"***, 2nd Edition, Pergamon, Oxford, 1982.

[2]-Report, **"*What is Heat Pipe?"***, Principle of heat pipe, (2005). Web site, (http://www. google.com), with key word, (what is heart pipe).

[3]- Hamdan et al, **"*Loop Heat Pipe (LHP) Development by Utilizing Coherent Porous Silicon (CPS) Wicks"***, Spacecraft Thermal Systems, NASA John H. Glenn Research Center at Lewis Field, 21000 Brookpark Road, Mail-Stop 301-2, Cleveland, Ohio, 44135 – 3191, University of Cincinnati, (2005). Web site, (http://www. google.com), with key word, (heart pipe + loop heat pipe).

[4]- Nikitkin M., and Cullimore B., ***"CPL and LHP Technologies: What are the Differences, What are the Similarities?"***, SAE Paper 981587, 1998.

[5]- Chandratilleke C., Hatakeyama H., and Nakagome H., ***"Development of Cryogenic Loop Heat Pipes"***, Cryogenics, Vol. 38, No. 3, pp. 263-269, 1998.

[6]- H_lke A., Henderson T., Gerner F., and Kazamierczak M., ***"Analysis of Heat Transfer Capacity of a Micro-machined Loop Heat Pipe"***, ASME Journal of Heat Transfer, submitted for publication, 1999.

[7]- Muraok I., Ramos F., and Vlassov V., ***"Experimental and Theoretical Investigation of a Capillary Pumped Loop with a Porous Element in the Condenser"***, *Int. Comm. Heat Mass Transfer*, Vol. 25, No. 8, pp. 1085-1094, 1998.

[8]- Muraoka, I.; Ramos, F.M.; Vlassov, V.V., ***"Analysis of the operational characteristics and limits of a loop heat pipe with porous element in the condenser"***,*International Journal of Heat and Mass Transfer*, Vol. 44, Issue: 12, pp. 2287-2297, 2001.

[9]- Schweickart R., Neiswanger L., and Ku J., 22nd AIAA ***Thermophysics Conference***, Honolulu, HI, paper AIAA 87-1630, 1987.

[10]- Swanson L., and Herdt G., ***"Model of the evaporating meniscus in capillary tube"***, ASME JOURNAL OF HEAT TRANSFER, Vol. 114, pp. 434-440, 1992.

[11]- Kaya T., and Hoang T., ***"Mathematical Modeling of Loop Heat Pipes and Experimental Validation"***, *J. of Thermo physics and* , Vol. 13, No. 3, pp. 314-320, 1999.

[12]- Figus C., Le Bray Y., Bories S., and Part M., ***"Heat and Mass Transfer with Phase Change in a Porous Structure Partially Heated: Continuum Model and Pore Network Simulations"***, *Int. J. of Heat and Mass Transfer*, Vol. 42, pp. 2557-2569, 1999.

[13]- Jentung Ku, ***"Operating Characteristics of Loop Heat pipes"***, 1999, 29th International Conference on Environmental system, Denver, Colorado, July 1999.

[14]- Kamotani Y., ***"Thermocapillary Flow Under Microgravity – Experimental Results",*** *Adv Space Res.*, Vol. 24, No. 10, pp 1357-1366, 1999.

[15]- Kandlikar S., Shoji M., Dhir V., ***"Handbook of phase change: boiling and condensation"***, Taylor & Francis, c1999.

[16]- Maidanik Y., Vershinin S., Kholodov V., and Dolggirev J., ***"Heat Transfer Apparatus"***, US patent 4515209, May 1985.

[17]- LaClair T., and Mudawar I., ***"Thermal Transients in Capillary Evaporator Prior to the Initiation of Boiling"***, Vol. 43, pp 3937-3952, 2000.

[18]- Kaya T., ***"Mathematical Modeling of Loop Heat Pipes and Experimenatl Validation"***, *J. of Thermophysics & Heat Transfer*, Vol. 13, No. 3, pp 314-320, 1999.

[19]- Gari, H.D., and Fathallah, K.A., ***"Modeling and Simulation of a Passive Condensate Heat Pipe Pumping System for Solar Energy Applications"*** Heat Recovery systems and Chp. 8 (6), 559-569(1988).

[20]- Po-Ya Abel Chuang ***"An Improved Steady State Model Of Loop Heat Pipes Based on Experimental And Theoretical Analyses"***, Thesis of Doctor of Philosophy from the Pennsylvania State University (2003). Web site, (http://www. google.com), with key word, (heart pipe + loop heat pipe).

[21]- Mertol, A., Place, W., Webster, T. and Grief, R.,***"Detailed Loop Model (DLM) Analysis of liquid solar Thermosyphons with Heat Exchangers"*** Solar Energy 27,367(1981).

[22]- Brun, G., ***"La re gularisation de l e nergie solaire par le stockage thermique dans le sol".Rev.Gen.Term.44 (1965).***

[23]- Roberts, C.C., Jr., ***"A Review of Heat Pipe Liquid Delivery Concepts"***, IV.Int.Heat Pipe Conf., Advances in Heat Pipe Technology (Edited by D.A.Reay), PP.693-697, Pergamon press, Oxford (1981).

[24]- ***"Passive Solar Heating and Cooling",*** Conf.And Workshop Proc.Rep.LA 667-C, Albuquerque, (Now Mexico) (1976).

[25]- Neeper, U. A. and Hedstorm, J. C.,***"A Self-Pumping Vapor System for Hybrid Space Heating"***, Cong. Int. Sol. Energy Soc., Monreal (June 1985).

[26]- Beni, G. D. and Friesen, R.***"Passive Downward Heat Transport: Experimental Results of a Technical Unit"***, Sol.Energy, 34,122-134(1985).

[27]- Gari, H. A., Akyurt, M. and Fathalah, K.A.F.,***"Investigation of a Very Long Heat Pipe"***, 2nd Technical Report AT-6-067,KACST,Riyadh,Oct.(1986).

[28]- Gari, H. A., and Fathalah, K.A.F.,***"Investigation of a Very Long Heat Pipe"***,3rd Technical Report AT-6-067,KACST,Riyadh,Dec.(1986).

[29]- Kern,D.Q.,***"Process Heat Transfer"***,PP.215(1950).

Properties of (R-114) and (R-11)

All of the working fluid properties are functions of liquid temperature and curve-fitted based on the data from ***"ASHARE HAND BOOK".*** These properties include saturation pressure, liquid density, liquid viscosity, vapor density, vapor viscosity, liquid thermal conductivity, vapor thermal conductivity, liquid specific heat, and vapor specific heat. They are expressed as a function of saturation temperature in the form of 5^{th}-order polynomial equations, and are (A-1) plotted in Figs. A_1 to A_{16}.

Physical properties of R-11

$$P=39830.3E\text{-}6+1860.12E\text{-}6*T+22.5873\,E\text{-}6*T^2+0.371842E\text{-}6*T^3 \quad \text{(A-1)}$$

$$\rho_f=1534.14-2.27015*T-0.00138177*T^2-1.76571E-5*T^3 \quad \text{(A-2)}$$

$$v_g=0.403131-0.0156709*T+3.332155E\text{-}4*T^2-4.24971E\text{-}6*T^3+2.972822E\text{-}8*T^4-8.57694E\text{-}11*T^5 \quad \text{(A-3)}$$

$$h_f=200.067+0.849659*T+0.639506E\text{-}3*T^2 \quad \text{(A-4)}$$

$$h_g=389.722+0.448958*T+5.04503E\text{-}3*T^2-0.128881E\text{-}3*T^3+0.00132038E\text{-}3*T^4-4.96792E\text{-}3*T^5 \quad \text{(A-5)}$$

$$\mu_g=1.01606E\text{-}5+3.44208E\text{-}8*T+6.35158E\text{-}12*T^2-4.72028E\text{-}13*T^3 \quad \text{(A-6)}$$

$$\mu_f=0.567513E\text{-}3-6.58856E\text{-}6*T+3.6109E\text{-}8*T^2-8.48099E\text{-}11*T^3 \quad \text{(A-7)}$$

$$C_{pg}=575.951E\text{-}3+1.29723E\text{-}3*T+0.304823E\text{-}5*T^2-4.46849E\text{-}8*T^3+5.24513E\text{-}10*T^4 \quad \text{(A-8)}$$

Physical properties of R-114

$$P=87197.2E\text{-}6+3668.52E\text{-}6*T+45.1998E\text{-}6*T^2+0.51257*T^3 \quad \text{(A-9)}$$

$$\rho_f=1505.25-1.63037*T-0.0258902*T^2+0.146388E\text{-}3*T^3-6.20537E\text{-}7*T^4 \quad \text{(A-10)}$$

$$v_g=0.145008-0.527681E\text{-}2*T-0.106421E\text{-}3*T^2-1.31952E\text{-}6*T^3+9.05342E\text{-}9*T^4-2.58174E\text{-}11*T^5 \quad \text{(A-11)}$$

$$h_f=200.021+0.951021*T+0.717245E\text{-}3*T^2 \quad \text{(A-12)}$$

$$h_g=333.129+0.582027*T+0.351506E\text{-}3*T^2-0.653068E\text{-}5*T^3 \quad \text{(A-13)}$$

$$\mu_g=1.04808E\text{-}5+4.61337E\text{-}8*T-2.6387E\text{-}10*T^2-4.72028E\text{-}12*T^3 \quad \text{(A-14)}$$

$$\mu_f=49.0745E\text{-}46.47185E\text{-}6*T+4.21317E\text{-}8*T^2-1.19853E\text{-}10*T^3 \quad \text{(A-15)}$$

$$C_{pg}=0.679909+1.33011E\text{-}3*T-0.0143474E\text{-}3*T^2+0.385393E\text{-}6*T^3 \quad \text{(A-16)}$$

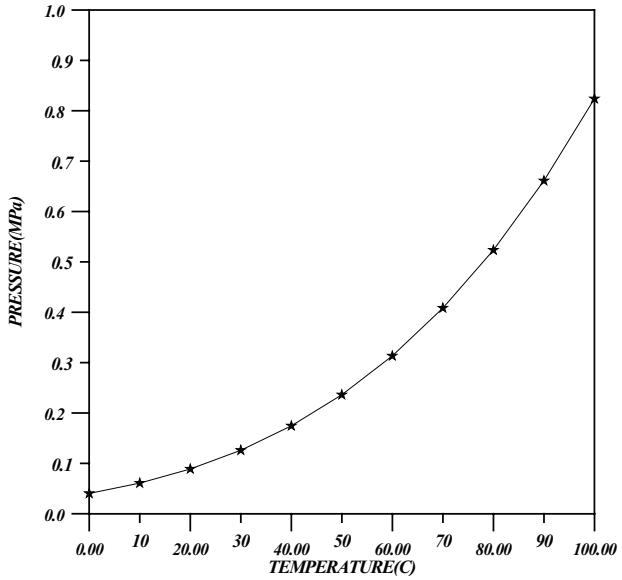

Fig.(A-1):pressure of Saturated R-11

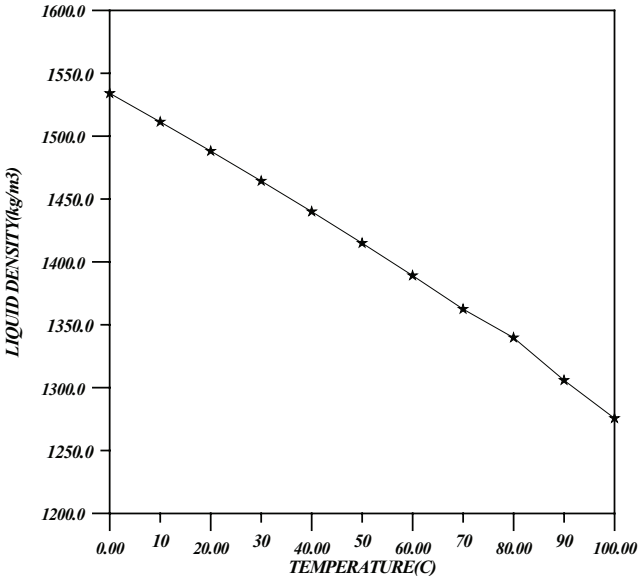

Fig.(A-2):Liquid density of Saturated R-11

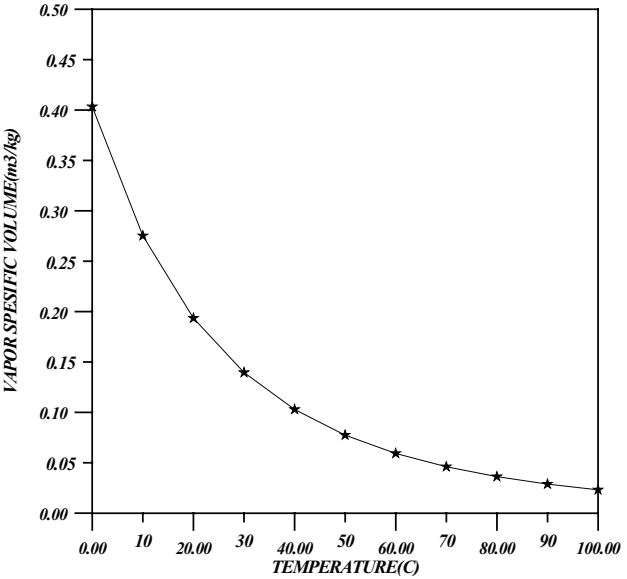

Fig.(A-3):Specific volume of Saturated R-11

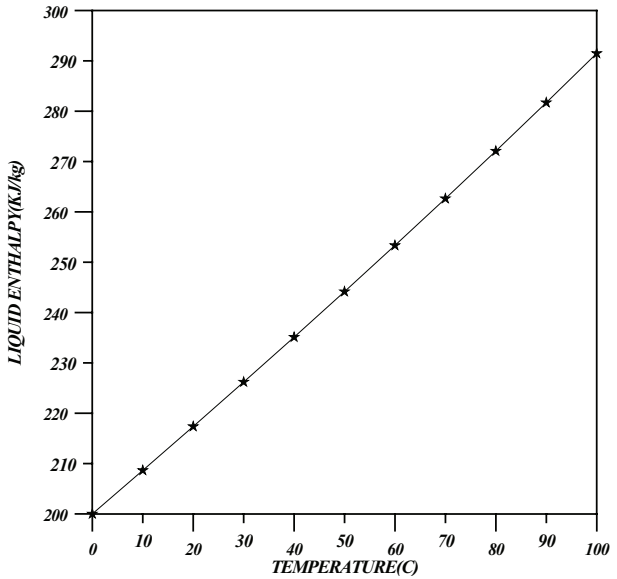

Fig.(A-.4):Liquid enthalpy of Saturated R-11

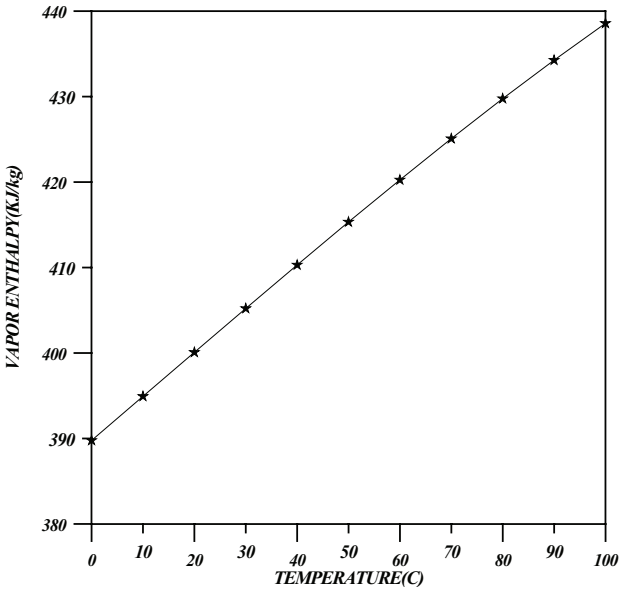

Fig.(A-5):Vapor enthalpy of Saturated R-11

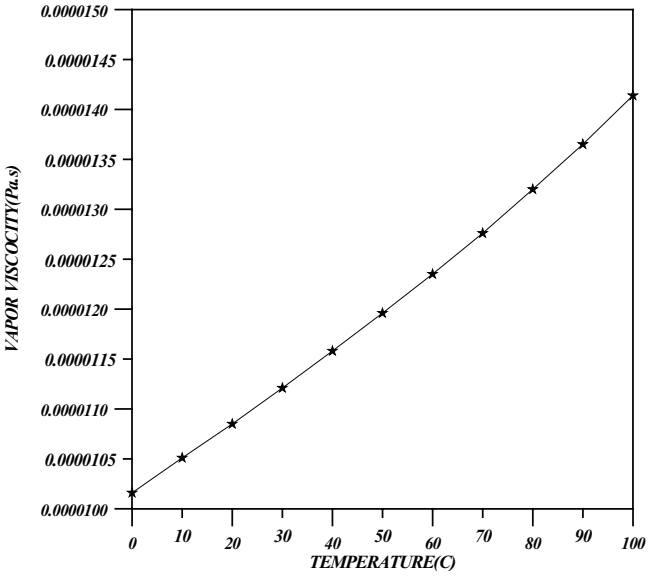

Fig.(A-6):Vapor viscosity of Saturated R-11

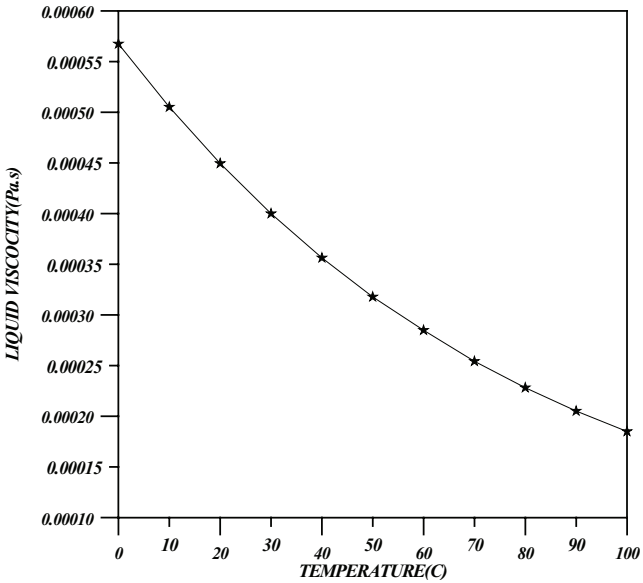

Fig.(A-7):Liquid viscosity of Saturated R-11

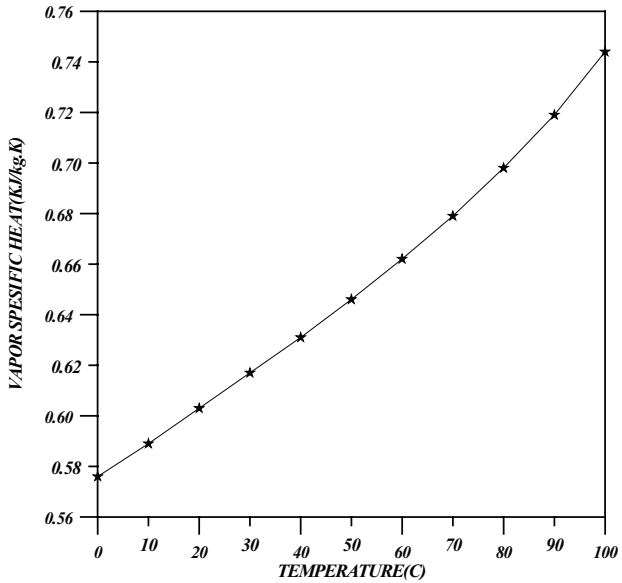

Fig.(A-8):Vapor specific heat of Saturated R-11

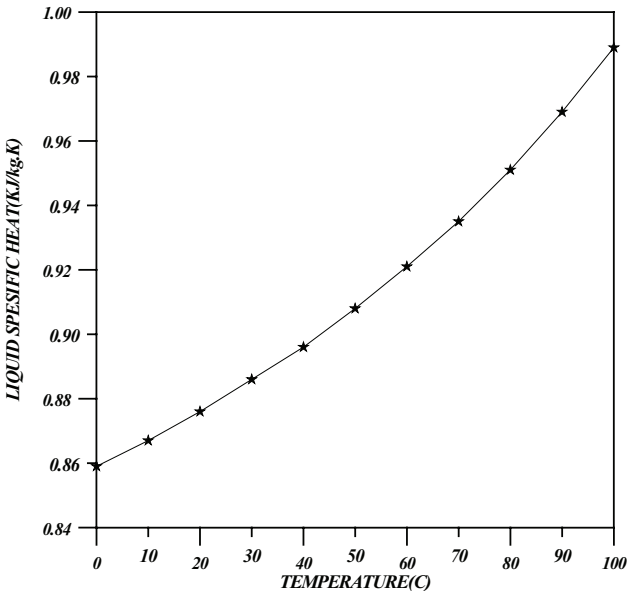

Fig.(A-9):Liquid specific heat of Saturated R-11

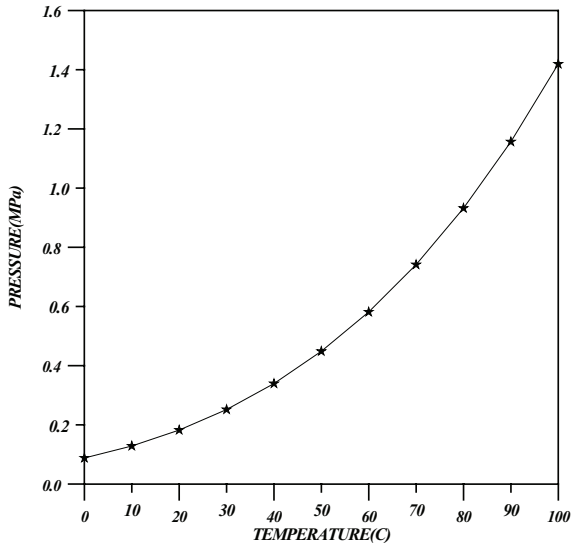

Fig.(A-10):Pressure of Saturated R-114

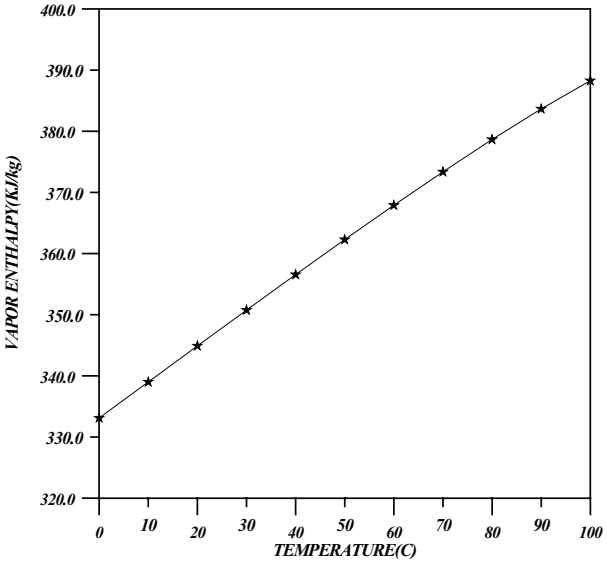

Fig.(A-11):Vapor enthalpy of R-114

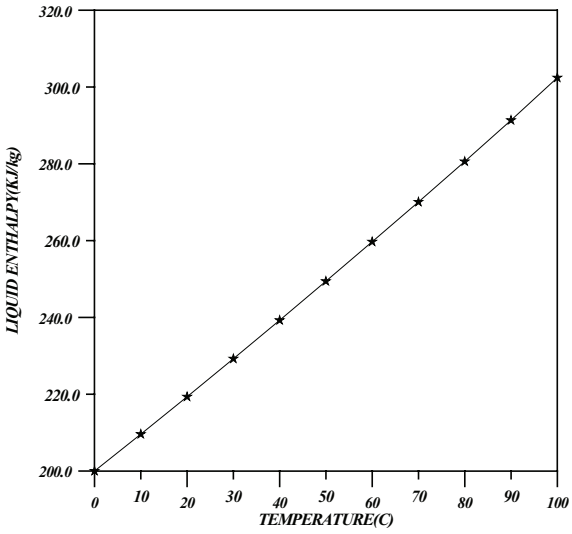

Fig.(A-12):Liquid enthalpy of Saturated R-114

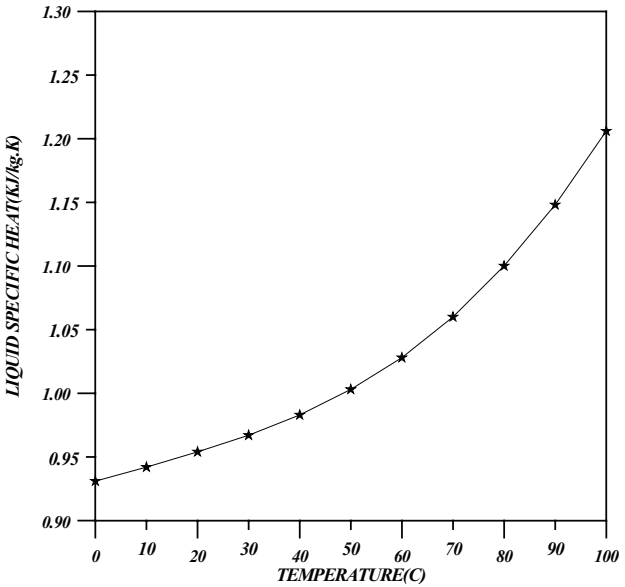

Fig.(A-13):Liquid specific heat of Saturated R-114

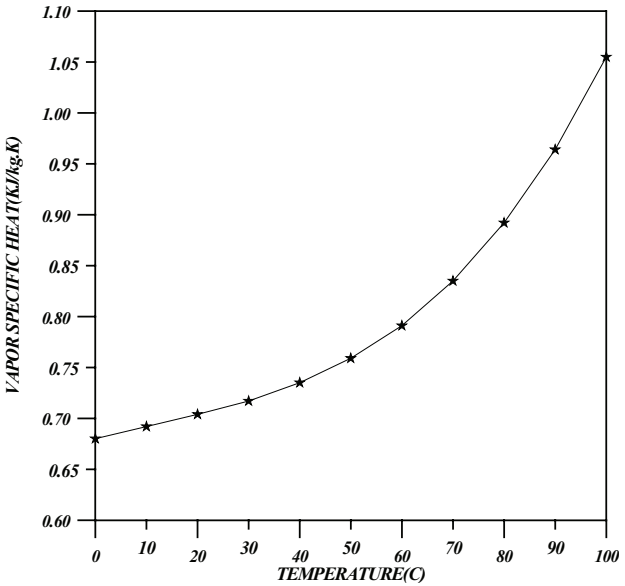

Fig.(A-14):Vapor specific heat of Saturated R-114

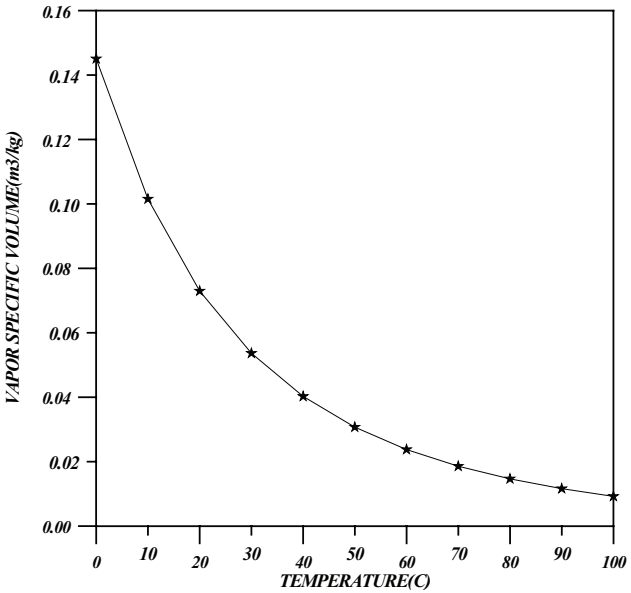

Fig.(A-15):Vapor specific volume of Saturated R-114

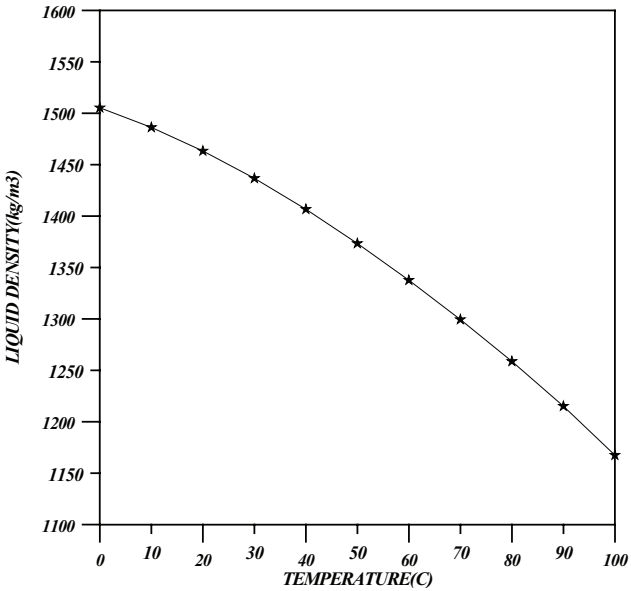

Fig.(A-16):Density of Saturated R-114

Numerical Method

Runge-Kutta method:

One of the important methods to solve the partial differential equations is ***"Runge-Kutta method"*** is more accuracy compared with Taylor series method, Euler's simple method, and Euler's trapezoidal method.

For example.

$$\frac{dy}{dx} = f(x,y) \ldots \text{(B.1)}$$

To solve Eq. (B.1) by ***Runge-Kutta methods*** can be getting the relation.

$$y_{n+1} = y_n + ak_1 + bk_2 \ldots \text{(B.2)}$$

Or

$$y_{n+1} = y_n + \Delta y$$

$$k_1 = h.f(x_n, y_n) \ldots \text{(B.3)}$$

$$k_2 = h.f(x_n + \alpha h, y_n + \beta k_1) \ldots \text{(B.4)}$$

Can be getting Eq. (B.2) coincided with Taylor series

$$y_{n+1} = y_n + h.f(x_n, y_n) + \left(\frac{h^2}{2}\right) f'(x_n, y_n) + \ldots \text{(B.5)}$$

Where

$$f' = \frac{df}{dx} = fx + fy\frac{dy}{dx}$$

But

$$f' = fx + fyf$$

Thus

$$y_{n+1} = y_n + h.f_n + \left(h^2\right)\left[\frac{fx}{2} + \frac{fyf}{2}\right]_n \ldots \text{(B.6)}$$

Can be written Eq. (B.2)

$$y_{n+1}=y_n+ah.f\left(x_n+y_n\right)+bh.f\left(x_n+\alpha h,y_n+\beta k_1\right)\ldots(B.7)$$

To getting the later term of Eq. (B.7) compared with Eq. (B.6)

$$f\left[\left(x_n+\alpha h,y_n,\beta h.f\left(x_n,y_n\right)\right)\right]=\left(f+fx\alpha h+fy\beta hf\right)_n \ \ldots(B.8)$$

The function [f] is partial function can be found by substituted Eq. (B.7) in Eq. (B.8) getting

$$y_{n+1}=y_n+ah.f_n+bh\left(f+fx\alpha h+fy\beta hf\right)_n$$

After arrangement getting

$$y_{n+1}=y_n+\left(a+b\right)h.f_n+h^2\left(\alpha bfx+\beta bfyf\right)_n \ldots(B.9)$$

And compared with Eq. (B.7) getting

$$a+b=1$$

$$\alpha b=\frac{1}{2}$$

$$\beta b=\frac{1}{2}$$

The final relation of Runge-Kutta is

$$y_{n+1}=y_n+\left(\frac{\left(k_1+2*k_2+2*k_3+k_4\right)}{6}\right)\ldots(B.10)$$

Where

$$k_1=h.f\left(x_n,y_n\right)$$

$$k_2=h.f\left(x_n+\frac{h}{2},y_n+\frac{k_1}{2}\right)$$

$$k_3=h.f\left(x_n+\frac{h}{2},y_n+\frac{k_2}{2}\right)$$

الخلاصه

طور النموذج الرياضي الشامل لمحاكاة سلوك نظام الضخ التحتي لناتج التكثيف الناقل للحرارة ألعابره. افترض بان شروط الإشباع تسود في جميع الأوقات في خليط (البخار–السائل) داخل المرجل.

نظام الأنبوب الحراري للتدوير الذاتي (**passive heat pipe system**) تم تحليله لمختلف الارتفاعات,الحرارة ألمسلطه على المرجل,نسبه تدفق الماء و السائل العامل.

افترض بان درجه حرارة المجمع (**accumulator**) تبقى قرب درجه الحرارة المحيط. إثناء عمليه الضخ يحدث نقل للحرارة بسبب (التبخر– التكثف) للسائل العامل. ناتج التكثف يدفع إلى المجمع نتيجة اختلاف الضغط بين المكثف والمجمع. المعادلات ألحاكمه(**mass conservation and energy conservation**) تم تطبيقها على النموذج و حلها.

برنامج الحاسوب يبنى لأداء الحل العددي (**numerical calculation**) للضغط و درجه حرارة المرجل و المكثف. كذلك برنامج الحاسوب يحسب ألكتله المدورة بين المرجل و المجمع. إن درجه حرارة ماء الخروج و كفاءة النظام تحسب أيضا. طريقه (**Range– Kutta**) تستعمل لحل المعادلات.

التأثيرات على سلوك النظام, السيطرة على خواص الديناميكا الحرارية الأكثر أهميه للسائل العامل, ومثال على ذلك:–الضغط, درجه الحرارة, الحرارة الكامنة لتبخر(**Latent heat of evaporation**), كثافة السائل و الحرارة ألنوعيه (**specific heat**) , يجب اختيار وعرض اقتراحات لاختيار السائل الصحيح للانظمه لمختلف(الارتفاعات, الكتل المدورة و الحرارة ألمسلطه).

الكفاءة المحسوبة في العمل الحالي, بالاضافه إلى الكفاءات المدروسة المتوفرة من دراسة الباحثين لنظام الضخ التحتي بناقل الحرارة المتفوق(بخار) وجد لكي يكون أكثر أو على الأقل مكافي للنظام التقليدي(**wick heat pipe**).

يلاحظ في العمل الحالي, تزايد درجه حرارة المرجل و المكثف عندما يزداد الحمل المسلط على المرجل. تزايد كفاءة النظام إثناء زيادة نسبه تدفق كتله ماء التبريد, ارتفاع المجمع و ألكتله المدورة بين المرجل و المجمع. أيضا يمكن إن يلاحظ ثلاثة مناطق إثناء تشغيل النظام, منطقه عدم الضخ(**no-pumping zone**) , ألمنطقه الانتقالية للضخ (**transional zone**) و منطقه الضخ(**pumping zone**). إن نتائج الفريون11عندما نستخدم الحرارة ألمسلطه على المرجل(2000w),الارتفاع بين المكثف و المجمع (15 m)و نسبه تدفق ماء التبريد (0.015 kg/s) تم التوصل إلى إن درجه حرارة المرجل,المكثف و الكفاءة هي: 89.3 , 81.17ºC, 90.78ºC, و لنفس الشروط أعلاه و لكن استخدام الفريون114نحصل على:64.4, 64.18ºC, 68.87ºC